iScience

CellPress
OPEN ACCESS

Article

The hypoxia-inducible factor EPAS1 is required for spermatogonial stem cell function in regenerative conditions

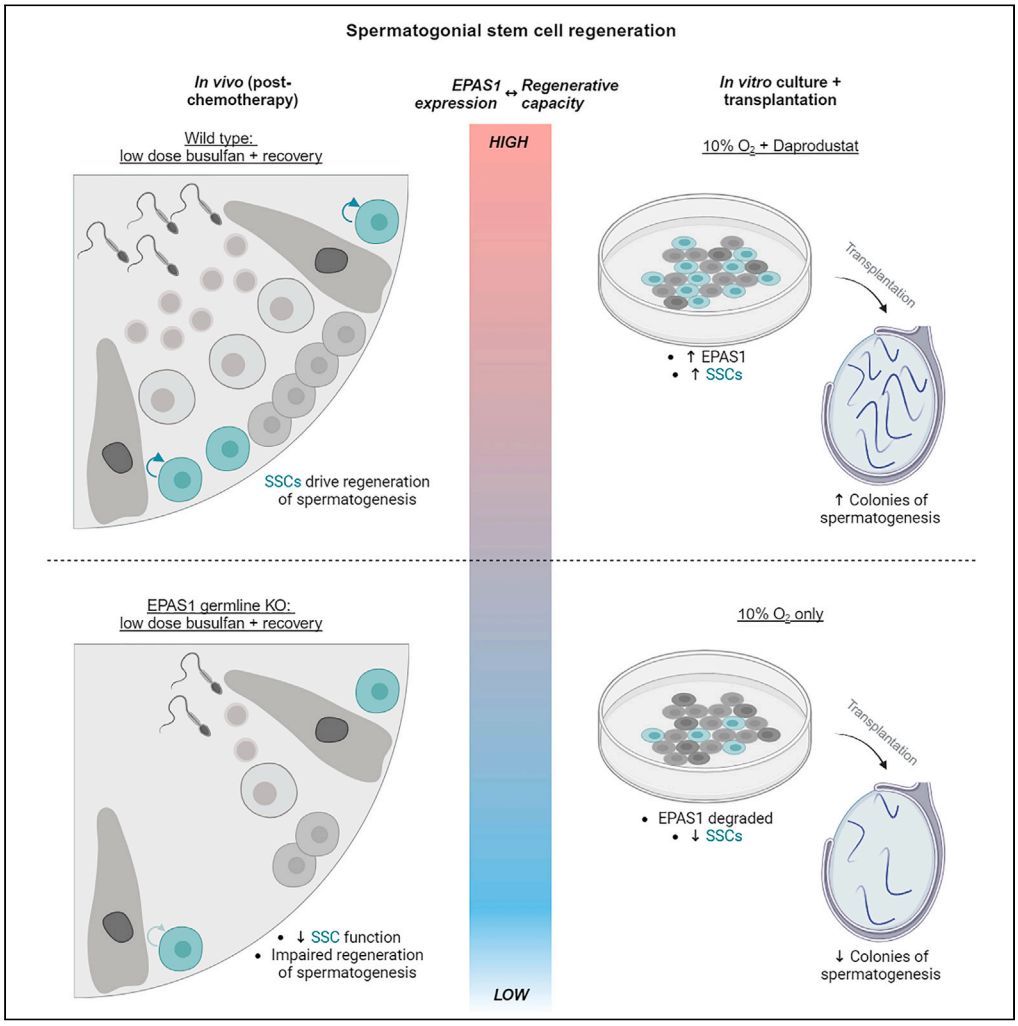

Ilana R. Bernstein, Brett Nixon, Jess M. Lyons, ..., Alyssa J. Lochrin, Jera L. Peters, Tessa Lord

tessa.lord@newcastle.edu.au

Highlights

Spermatogonial stem cells (SSCs) reside in hypoxic niches in the testes

Ablation of the hypoxic factor EPAS1 impairs SSC regeneration after chemotherapy

Stabilizing EPAS1 expression in culture improves SSC maintenance

Bernstein et al., iScience *26*, 108424
December 15, 2023
https://doi.org/10.1016/j.isci.2023.108424

iScience

CellPress
OPEN ACCESS

Article

The hypoxia-inducible factor EPAS1 is required for spermatogonial stem cell function in regenerative conditions

Ilana R. Bernstein,[1] Brett Nixon,[1,2] Jess M. Lyons,[1] Katerina B. Damyanova,[1] Camila S. De Oliveira,[1] Nishani S. Mabotuwana,[1] Simone J. Stanger,[1] Gerard E. Kaiko,[3,4] Tan Hui Ying,[3,4] Jon M. Oatley,[5] Nicole M. Skillen,[1] Alyssa J. Lochrin,[1] Jera L. Peters,[1] and Tessa Lord[1,2,6,*]

SUMMARY

In this study we explored the role of hypoxia and the hypoxia-inducible transcription factor EPAS1 in regulating spermatogonial stem cell (SSC) function in the mouse testis. We have demonstrated that SSCs reside in hypoxic microenvironments in the testis through utilization of the oxygen-sensing probe pimonidazole, and by confirming the stable presence of EPAS1, which is degraded at >5% O_2. Through the generation of a germline-specific *Epas1* knockout mouse line, and through modulation of EPAS1 levels in primary cultures of spermatogonia with the small drug molecule Daprodustat, we have demonstrated that EPAS1 is required for robust SSC function in regenerative conditions (post-transplantation and post-chemotherapy), via the regulation of key cellular processes such as metabolism. These findings shed light on the relationship between hypoxia and male fertility and will potentially facilitate optimization of *in vitro* culture conditions for infertility treatment pipelines using SSCs, such as those directed at pediatric cancer survivors.

INTRODUCTION

Stem cells rely on a niche microenvironment to provide extrinsic cues that orchestrate self-renewal and maintenance of the population. In a majority of adult stem cell systems such as those of hematopoietic and neuronal lineages, the niche is relatively well defined, with one distinct characteristic being low oxygen tension (~1% O_2, reviewed by Jež et al.[1]). In these stem cells, hypoxia-inducible transcription factors (HIFs) drive expression of pluripotency genes and key cellular processes such as glycolytic metabolism that are actively required for stem cell maintenance (reviewed by Lord and Nixon[2]). On the other hand, the transition away from a stem cell state toward progenitor formation and differentiation is accompanied by cellular relocation to higher-oxygen environments in these tissues (~6–8% O_2,[1]), which causes a cessation of HIF signaling.

Within the HIF family of transcription factors, protein stability of the HIF-alpha subunits (HIF1A, HIF2A/EPAS1, and HIF3A) is directly regulated by oxygen availability, while the HIF-beta subunit (ARNT) is stable and ubiquitous.[3] In oxygen concentrations ≥5% or 36 mmHg, HIF-alpha proteins become hydroxylated (by prolyl hydroxylases, EGLN1-3) and ubiquitinated (facilitated by the von Hippel-Lindau protein [VHL]), targeting them for degradation by the proteasome.[3–5] Dimerization between a HIF-alpha subunit and ARNT is required to achieve promotor/enhancer binding to hypoxia-responsive elements;[6] thus, HIF signaling is ablated with HIF-alpha degradation in "high oxygen" conditions. Notably, although HIF1A and EPAS1 do share common target genes, they are also known to drive expression of unique sets of genes and signaling pathways,[7] accounting for the differences in associated phenotypes that will be discussed below. HIF3A is dissimilar from HIF1A and EPAS1 in that it lacks the c-terminal transactivation domain required to recruit co-transcriptional regulators and basal transcriptional machinery.[8]

Although a role for hypoxia and HIF signaling in regulating stem cell function is well defined in a number of tissue types, their involvement in regulating spermatogonial stem cell (SSC) activity is poorly understood. This is, in part, because SSCs reside in an "open niche" microenvironment along the perimeter of the basement membrane, rather than a more traditional "closed niche" structure.[9] Despite this, gradients of oxygen concentration exist based on the distance of cells from vasculature that is interspersed throughout the testis in the interstitial space. Where the SSCs reside in terms of vicinity to the interstitial space has been the subject of conflicting data (reviewed by Lord and Nixon[2]) but,

[1]Priority Research Centre for Reproductive Science, Discipline of Biological Sciences, The University of Newcastle, Callaghan, NSW 2308, Australia
[2]Hunter Medical Research Institute, Infertility and Reproduction Program, New Lambton Heights, NSW 2305, Australia
[3]Hunter Medical Research Institute, Immune Health Research Program, New Lambton Heights, NSW 2305, Australia
[4]School of Biomedical Sciences and Pharmacy, College of Health and Medicine, The University of Newcastle, Callaghan, NSW 2308, Australia
[5]School of Molecular Biosciences, Centre for Reproductive Biology, College of Veterinary Medicine, Washington State University, Pullman, WA 99164, USA
[6]Lead contact
*Correspondence: tessa.lord@newcastle.edu.au
https://doi.org/10.1016/j.isci.2023.108424

regardless, is likely an oversimplified readout of oxygen availability when considering the broad range in vasculature size throughout the testis, and the fact that functional vasculature is not apparent within every segment of the interstitium.[10]

Encouragingly, several studies have suggested a potential role for HIFs in male fertility and SSC function, particularly EPAS1, for which global knockout mice (*Epas1*$^{-/-}$) exhibit complete infertility.[11] In subsequent studies where *Epas1* expression was ablated at postnatal day 2 (*Epas1*$^{fl/fl}$, *Ubc-CreER*^{T2}) to exclude any secondary effects on the phenotype from impaired embryogenesis,[12,13] male mice exhibited a progressive loss of germ cells with age. Although this was attributed to Sertoli cell dysfunction and disruption to the blood-testis-barrier, assessments of testis histology at 4 and 13 months of age reveal seminiferous tubules that are completely devoid of germ cells, a phenotype that is reminiscent of an SSC self-renewal defect.[14] In the case of HIF1A, inducible knockout at postnatal day 2 did not have any discernible effects on spermatogenesis,[12] and traditional global knockout models are embryonic lethal.[15] Thus, given that ARNT ablation phenocopies EPAS1 ablation with inducible knockout at postnatal day 2,[12] it is apparent that EPAS1/ARNT dimerization, rather than HIF1A/ARNT dimerization, drives HIF signaling pathways that are important for spermatogenesis.

In considering evidence for a role for HIF signaling in germline stem cells specifically, our own work utilizing a large-scale RNAi screen identified this pathway as a candidate for regulating SSC maintenance,[16] with knockdown of several auxiliary transcription factors instigating a loss of *Id4-eGfp*-expressing putative stem cells.[17] Additionally, in a recent review of single-cell RNA sequencing (scRNA-seq) databases that capture spermatogonia from the mouse and human testis, we revealed that SSCs possess a transcriptomic signature that is reminiscent of a hypoxic cell,[2] expressing elevated levels of genes involved in glycolytic metabolism that are known to contain hypoxia-responsive elements in their promotor region (e.g., *Aldoa*, *Pkm*, *Gapdh*). Beyond this, hypoxia has been found to be a factor influencing apoptosis of undifferentiated spermatogonia in a mouse line carrying a Dead end 1 (*Dnd1*) mutation that sensitizes germ cells to spermatogenic failure and teratomas.[18] Finally, a recent manuscript that used transcriptomics to investigate the SSC expression profile in regenerative conditions identified HIF signaling as a potential driver of SSC proliferation post-chemotherapy treatment.[19]

In this study we investigated the notion of a hypoxic stem cell niche in the mouse testis and explored the role of EPAS1 in regulating SSC function and male fertility. Using an *Id4-eGfp* transgenic mouse model to identify SSCs,[17,20] we were able to assess expression of HIF-alpha proteins and perform *in situ* studies with the oxygen-sensing probe pimonidazole to confirm that a vast majority of SSCs (>80%) do reside in hypoxic conditions in the testis. Coinciding with this, we identified that disruption to normal EPAS1-driven signaling pathways occurs when maintaining SSCs in culture, and that preventing EPAS1 degradation with the prolyl hydroxylase inhibitor Daprodustat significantly improves SSC maintenance *in vitro*. In generating an *Epas1* conditional knockout mouse line (EPAS1-cKO) where *Epas1* ablation was specific to the germ cells, it was determined that, although EPAS1 is not absolutely required for SSC maintenance in steady-state conditions, loss of expression does instigate a reduction in sperm output, motility, and viability, corresponding with modest reductions in fertility. However, EPAS1 expression was found to be required for SSC function in regenerative conditions, to facilitate unimpaired regeneration of the undifferentiated spermatogonia pool, and downstream spermatogenesis, post-chemotherapy treatment.

RESULTS

SSCs exist in hypoxic microenvironments in the testis

In a cell population existing in hypoxia, it is expected that at least a subset of HIF-alpha subunits will be expressed to modulate downstream gene expression and cell survival. To begin to explore HIF expression in SSCs versus downstream spermatogonial subsets, we firstly examined transcript levels using a previously published scRNA-seq dataset from PD6 mouse testes (Law et al.,[21] GEO accession number GSE124904). SSC, progenitor, and differentiating spermatogonia populations were identified and delineated based on their well-characterized gene expression profiles (Figures S1A and S1B and as published previously.[21,22]) Specifically, SSCs were identified by the expression of key markers such as *Gfra1*, *Etv5*, *Id4*, and *Plvap*, progenitors by their expression of *Neurog3*, *Sohlh1*, and *Sox3*, and differentiating spermatogonia by expression of *Stra8* and *Kit* (Figure S1B and complete list of cluster identifiers in Data S1). In assessing HIF-alpha genes in SSCs, both *Hif1a* and *Epas1* were expressed, while expression of *Hif3a* was negligible. Interestingly, downregulated expression of *Epas1* and *Hif1a* was identified along the trajectory from SSC to differentiating spermatogonia (Figure S1C, upper), a finding that is supported by other previously published scRNA-seq databases (reviewed previously by Lord and Nixon[2]), including significant enrichment of *Epas1* in undifferentiated spermatogonia in the adult mouse testis,[22] and in primitive SSC populations ("State 0") from the adult human testis.[23,24] In contrast to HIF expression, expression of genes that orchestrate the degradation of HIF-alpha proteins in normoxic conditions (*Egln1-3*, *Vhl*, and *Hifan*) showed lowest levels of expression in the SSC population, with upregulation upon the progenitor and differentiating transitions (Figure S1C, lower).

Although the mRNA expression profile is informative, the functionality of HIF-alpha pathways is reliant on protein stability, given that these proteins will be hydroxylated, ubiquitinated, and degraded in O_2 conditions $\geq$5% or 36 mmHg.[3–5] Thus, we next explored expression of HIF1A and EPAS1 in SSC and progenitor populations, using an *Id4-eGfp* transgenic mouse line[17,20] in which spermatogonia with high levels of transgene expression (ID4-EGFP^{Bright}) have been shown to comprise a veritably pure population of SSCs, while the ID4-EGFP$^{Dim/Negative}$ population largely comprises progenitor spermatogonia.[17,20] In assessing testis sections from both PD6 and adult mice, it was observed that HIF1A had increased protein stability in ID4-EGFP^{Bright}-labeled SSCs when compared to progenitor spermatogonia (Figures S1D and S1E). Specifically, 81% ($\pm$15.5) of SSCs in the PD6 testis (Figure S1D) and 89% ($\pm$6.1) in the adult testis (Figure S1E) showed HIF1A expression, compared to 9% ($\pm$11.3) and 2.5% ($\pm$1.3) of progenitors, respectively ($p < 0.05$ and $p < 0.01$). In assessing EPAS1, it was apparent that protein expression was again almost exclusive to the ID4-EGFP-labeled SSCs (Figures 1A and 1B). In the PD6 testis, 95% ($\pm$5.0) of SSCs were EPAS1+, compared to only 6.5% of progenitors ($\pm$1.3) ($p < 0.01$) (Figure 1A), a trend that was replicated in the adult testis (Figure 1B, 100% versus 4.3% ($\pm$1.8), $p < 0.001$). Given our particular interest in EPAS1, we further confirmed these results via immunoblotting using ID4-EGFP^{Bright} and ID4-

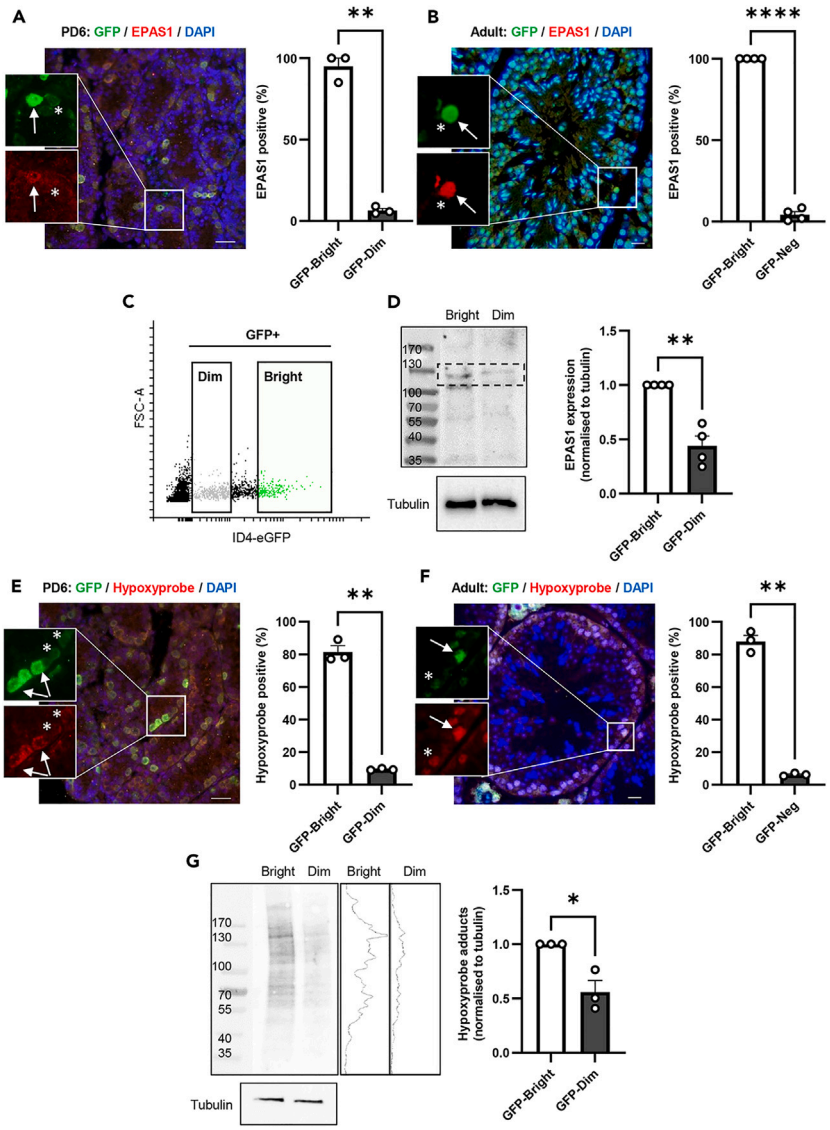

Figure 1. Spermatogonial stem cells exist in hypoxic microenvironments in the testis

(A) (*Left*) Immunofluorescence analysis of EPAS1 expression (red) in a PD6 *Id4-eGfp* transgenic mouse testis. GFP-Bright cells are SSCs (white arrow), and GFP-Dim cells are progenitor spermatogonia (white asterisk). DAPI (blue) was used as a nuclear stain. Scale bar = 20 μm. *(Right)* Quantitative assessment of the percentage of GFP-Bright and GFP-Dim spermatogonia that were found to be expressing EPAS1. Histogram depicts mean ± SEM for n = 3 biological replicates. ** denotes significantly different at $p < 0.01$ (t test).

(B) (*Left*) Immunofluorescence analysis of EPAS1 expression (red) in an adult (6–8 week old) *Id4-eGfp* transgenic mouse testis. GFP-Bright cells are SSCs (white arrow) and GFP-Dim/negative cells represent the progenitor transition onwards (white asterisk). *(Right)* Quantitative assessment of the percentage of GFP-Bright and GFP-Dim/negative spermatogonia that were found to be expressing EPAS1 (n = 4, $p < 0.001$ (t test)).

(C) Gating parameters for FACS isolation of ID4-EGFP-Bright SSCs and ID4-EGFP-Dim progenitor spermatogonia from a PD6 mouse testes.

(D) (*Left*) Immunoblot depicting EPAS1 expression (118 kDa) in lysates from FACS sorted ID4-EGFP-Bright SSCs and ID4-EGFP-Dim progenitor spermatogonia (PD6 testes). Lower is Tubulin loading control. *(Right)* Densitometry analysis of EPAS1 expression, normalized to Tubulin (n = 4, $p < 0.01$ (t test)).

(E) (*Left*) Immunofluorescence analysis of Hypoxyprobe (pimonidazole) adduct formation (red) in a PD6 *Id4-eGfp* transgenic mouse testis. GFP-Bright cells are SSCs (white arrow), and GFP-Dim cells are progenitor spermatogonia (white asterisks). *(Right)* Quantitative assessment of the percentage of GFP-Bright and GFP-Dim spermatogonia that were found to exhibit high levels of pimonidazole adducts (strong red fluorescence) (n = 3, $p < 0.01$ (t test)).

(F) (*Left*) Immunofluorescence analysis of Hypoxyprobe (pimonidazole) adduct formation (red) in an adult *Id4-eGfp* transgenic mouse testis. GFP-Bright cells are SSCs (white arrow) and GFP-Dim/negative cells represent the progenitor transition onwards (white asterisk). *(Right)* Quantitative assessment of pimonidazole adducts in GFP-Bright and GFP-Dim/negative spermatogonia (n = 3, $p < 0.01$ (t test)).

(G) (*Left*) Immunoblot depicting Hypoxyprobe adducts in ID4-EGFP-Bright SSCs and ID4-EGFP-Dim progenitor spermatogonia from PD6 mouse testes. Right hand panel is a trace analysis of adduct formation. Lower is Tubulin loading control. Images depicting non-pimonidazole injected and whole testis controls are provided in Figure S1G. *(Right)* Densitometry analysis of Hypoxyprobe adduct formation, normalized to Tubulin (n = 3, $p < 0.05$ (t test)).

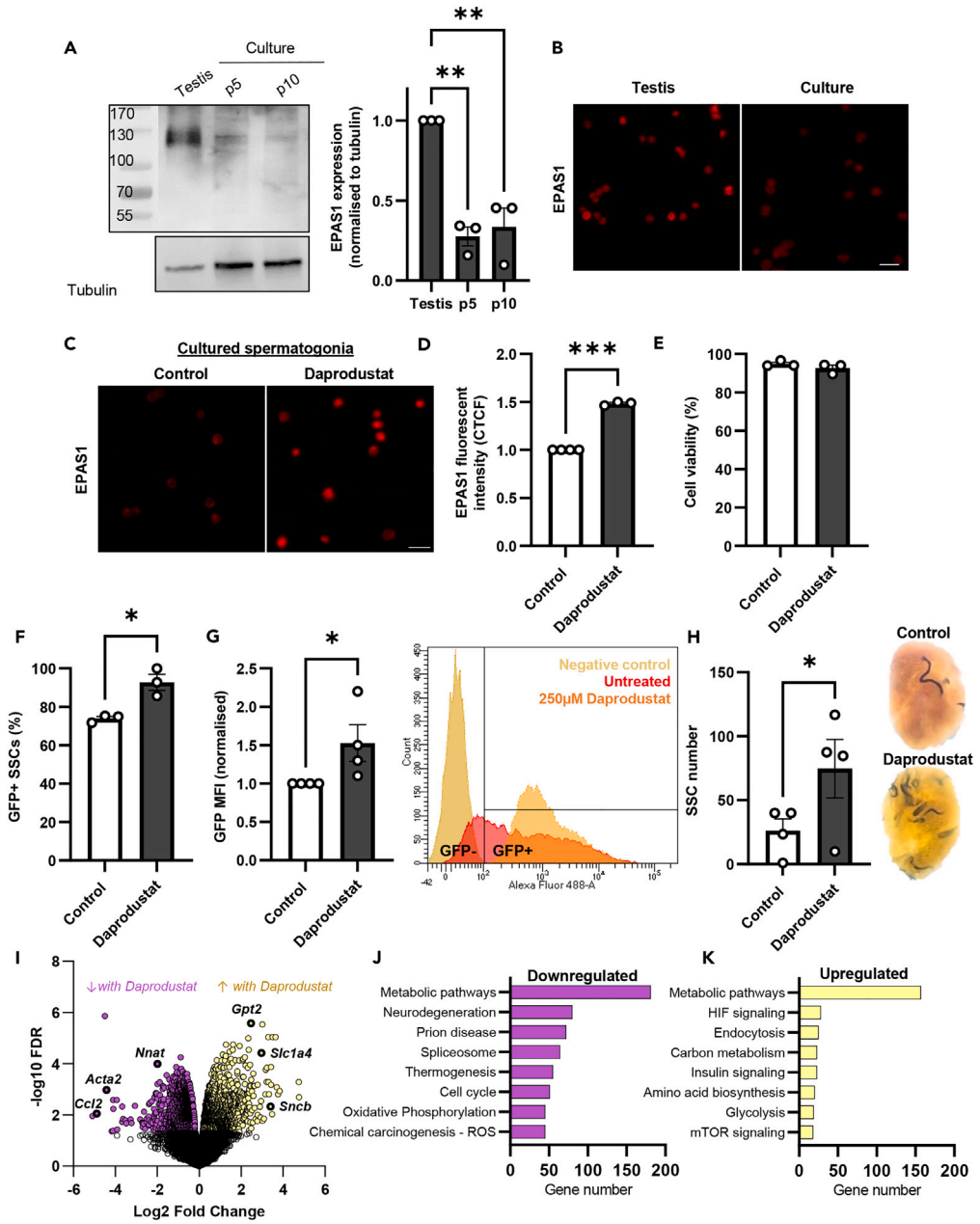

Figure 2. HIF signalling pathways are important for normal SSC function and are dysregulated in standard *in vitro* culture conditions

(A) (*Left*) Immunoblot depicting EPAS1 expression (118 kDa) in lysates from undifferentiated spermatogonia collected from the testis (ID4-EGFP+ population, PD6 testis), or from primary culture after 5 or 10 passages. Lower is Tubulin loading control. (Right) Densitometry analysis of EPAS1 expression, normalized to Tubulin. Histogram depicts mean ± SEM for n = 3 biological replicates. ** denotes significantly different at $p < 0.01$ (ANOVA).

(B) Immunofluorescence images accompanying (A), depicting reduced EPAS1 expression (red) in undifferentiated spermatogonia following 10 passages in *in vitro* culture versus undifferentiated spermatogonia collected directly from a PD6 testis. Scale bar = 20 μm.

(C) Immunofluorescence images depicting increased EPAS1 expression (red) in undifferentiated spermatogonia from culture following 24 h exposure to 250 μM Daprodustat, as compared to a vehicle (DMSO) control. Scale bar = 20 μm.

(D) Quantification of corrected total cell fluorescence (CTCF) of EPAS1 expression comparing undifferentiated spermatogonia from culture following 24 h exposure to 250 μM Daprodustat (n = 4, $p < 0.001$ (t test)), as compared to a vehicle (DMSO) control (accompanying images in (C), and dose response studies in Figure S2).

(E) Cell viability (Live/dead flow cytometry assay) of undifferentiated spermatogonia from culture following 24 h exposure to 250 μM Daprodustat or vehicle (DMSO control) (n = 4).

Figure 2. *Continued*

(F and G) Assessment of the percentage of ID4-EGFP+ cells (F) and mean fluorescence intensity (MFI) (G) in undifferentiated spermatogonia from culture following 24 h exposure to 250 μM Daprodustat, as compared to a vehicle (DMSO) control (n = 3–4, $p < 0.01$ (t test)). FACS plot in (G) shows ID4-EGFP expression alongside a negative control with no GFP transgene.

(H) Spermatogonial transplantation analysis depicting the number of donor-derived colonies of spermatogenesis formed per 10^5 cells transplanted ("SSC number") from cultured undifferentiated spermatogonia treated with either DMSO (control) or 250 μM Daprodustat (n = 4, $p < 0.05$ (t test)).

(I) Bulk RNA-seq analysis comparing undifferentiated spermatogonia from culture treated with either DMSO or 250 M Daprodustat. Downregulated genes denoted by purple circles and upregulated genes denoted by yellow circles had a false discovery rate (FDR) of $p < 0.05$.

(J) Gene Ontology (GO) analysis of genes that were significantly downregulated following Daprodustat treatment (I). Pathways highlighted here were significantly enriched at $p < 0.05$.

(K) GO analysis of genes that were significantly upregulated following Daprodustat treatment (I). Pathways highlighted here were significantly enriched at $p < 0.05$.

$EGFP^{Dim}$ populations that had been isolated via fluorescence-activated cell sorting (FACS) using gating parameters depicted in Figure 1C. Immunoblotting and accompanying densitometry analyses (normalized to tubulin) depicted a 50% reduction in EPAS1 expression (118 kDa) in progenitor spermatogonia when compared to SSCs ($p < 0.01$, Figure 1D).

To further establish the existence of a hypoxic SSC niche in the testis, we also utilized a Hypoxyprobe Kit for *in situ* analyses. In these analyses, the oxygen-sensing compound pimonidazole (2-nitroimidazole) was administered to *Id4-eGfp* mice via intraperitoneal injection. Pimonidazole becomes reduced only within cells that reside in hypoxic environments (<1.3% O_2),[25] forming stable thiol-adducts that can be detected using an anti-pimonidazole antibody. Immunofluorescence analyses were performed on *Id4-eGfp* testes from Hypoxyprobe-treated mice (Figures 1E and 1F; Figure S1H for control images) and on FACS-isolated spermatogonia populations (Figure S1F). In both cases, fluorescence associated with Hypoxyprobe adducts was visibly elevated in $EGFP^{Bright}$ SSCs. In the PD6 testis, 81.4% (±3.8) of SSCs showed Hypoxyprobe adducts (Figure 1E, red fluorescence, white arrows), compared to only 9.4% (±0.3) of progenitors ($p < 0.01$). Similarly, in the adult testis, 88% (±3.7) of SSCs exhibited Hypoxyprobe adduct formation (Figure 1F), compared to only 6.2% (±0.5) of progenitors ($p < 0.01$). FACS-isolated $EGFP^{Bright}$ and $EGFP^{Dim}$ populations from PD6 Hypoxyprobe-treated males were also assessed using immunoblotting analyses (Figure 1G and Hypoxyprobe versus untreated control images in Figure S1G). Again, significantly higher levels of pimonidazole adducts ($p < 0.05$) were identified in SSCs when compared to progenitor spermatogonia (Figure 1G), as depicted by densitometry analysis normalized to tubulin. Pimonidazole adducts were observed in proteins of all sizes in SSC lysates; however, they were particularly prominent in proteins of molecular weight 50–170 kDa (Figure 1G). Cumulatively, these results suggest that SSCs in the mouse testis reside in hypoxic microenvironments and are subjected to HIF1A and EPAS1 signaling pathways, which begin to decline upon the progenitor transition.

HIF signaling pathways are important for normal SSC function and are dysregulated in standard *in vitro* culture conditions

Upon confirmation that SSCs in the testis reside in hypoxic niches and express HIF-alpha proteins, we next endeavored to explore the influence of these proteins on SSC gene expression and function. EPAS1 was selected as our candidate of primary interest because 1) *EPAS1* expression is conserved in human SSCs[23] and 2) *Epas1* global knockout male mice have been previously reported to experience infertility,[11] while *Hif1a* deletion does not create a discernible male infertility phenotype.[12,26] In concert with our interest in identifying the functional role of EPAS1 in SSCs, we hypothesized that primary cultures of undifferentiated spermatogonia would be an extremely useful model, given that they are maintained at 10%–20% O_2,[27] which should instigate EPAS1 degradation. Accordingly, we hypothesized that loss of EPAS1 expression is associated with the decline in SSC function that is observed with prolonged culture time *in vitro*.[27]

To confirm that EPAS1 expression was significantly diminished in SSCs in culture, immunoblotting (Figure 2A) and immunofluorescence (Figure 2B) analyses were performed. As expected, a significant decline in EPAS1 expression was observed when comparing undifferentiated spermatogonia populations maintained in culture for 5 or 10 passages (5% CO_2, 10% O_2,[16]) to those isolated directly from the testis (ID4-EGFP+ cells) (Figure 2A, $p < 0.01$). Upon this confirmation, we endeavored to restore normal EPAS1 signaling in a subset of undifferentiated spermatogonia *in vitro* and observe the consequences on SSC function and gene expression. To achieve this, undifferentiated spermatogonia that had been cultured for 10+ passages were treated with the prolyl-hydroxylase (EGLN) inhibitor Daprodustat, which instigated a consistent and significant dose-dependent increase in EPAS1 expression (Figures 2C, 2D and S2A) but not HIF1A expression (Figures S2B and S2C), with no effect on cell viability (Figure 2E). In alignment with our hypothesis that EPAS1 expression contributes to regulating stem cell function, Daprodustat treatment caused a significant elevation in the percentage of ID4-EGFP+ cells within the culture well ($p < 0.05$, Figure 2F) and the mean fluorescence intensity of EGFP ($p < 0.05$, Figure 2G) after only 24 h of treatment. Further, transplantation analyses confirmed a significant increase in the number of SSC-derived colonies of spermatogenesis following transplantation of Daprodustat-treated spermatogonia versus control spermatogonia (3-fold change, $p < 0.05$, Figure 2H), confirming a role for EPAS1 in the normal function of SSCs in regenerative conditions.

To identify SSC genes and molecular pathways that are regulated by EPAS1 expression, a bulk RNA sequencing (RNA-seq) comparison of control and Daprodustat-treated undifferentiated spermatogonia was also performed (n = 4). Imposing a false discovery rate (FDR) cutoff of <0.05, 3,604 genes were found to be differentially expressed, 1,759 upregulated following Daprodustat treatment (582 with a fold change ≥2) and 1,845 downregulated (276 with a fold change ≤ -2) (Figure 2I and Data S2). To provide an overview of key cellular process controlled by these genes, Gene Ontology (GO) analysis was performed. Within the downregulated gene list, significantly enriched pathways ($p < 0.05$) were largely associated with metabolism (specifically oxidative phosphorylation), protein homeostasis (i.e., prion disease, proteasome, and neurodegeneration),

and the cell cycle (Figure 2J and Data S2). Within the upregulated gene list, significantly enriched pathways ($p < 0.05$) included HIF signaling, metabolism (specifically glycolysis), insulin signaling, and mammalian target of rapamycin (mTOR) signaling (Figure 2K and Data S2).

Exploring the effects of *Epas1* ablation in SSCs *in vivo* in steady-state conditions

To next investigate the effects of *Epas1* ablation on male fertility and SSC function in steady-state conditions, a germline-specific knockout was generated using previously established *Ddx4(Vasa)*-Cre[28] and *Epas1*-fl mouse lines.[13] In these EPAS1-cKO males, exon 2 is deleted from germ cells (Figures S3A–S3C) from embryonic day ~15.5,[28] ablating the DNA-binding bHLH domain.[13] In observing hematoxylin and eosin (H&E)-stained testes at PD6, it was confirmed that the spermatogonial pool formed normally in the EPAS1-cKO (Figure S3D). In a breeding study in which control, heterozygous, and cKO males were paired with control females up to 6 months of age, a significant reduction in the number of pups sired per male was identified in the cKO as compared to the control (30 ± 5.4 versus 49.5 ± 3.7, respectively, $p < 0.05$, Figure 3A). There was no significant difference in the number of litters sired per male (Figure 3B). To establish whether any further exacerbation of this mild sub-fertility defect occurred with age, a longer-term breeding study was performed in which heterozygous and cKO males up to 12 months of age were paired with control females (periodically replaced so they were consistently <6 months of age). No increase in severity of the phenotype was identified, although EPAS1-cKO males again sired less pups over the breeding period (59 ± 20.3 compared to 85 ± 2.9 for heterozygous males, $p = 0.1$, Figure S3E), and the total number of litters produced by cKO males was reduced (9.7 ± 1.7 versus 12.5 ± 0.3 for heterozygous males, $p = 0.053$, Figure S3F).

In assessing control, heterozygous, and cKO males at 2 months of age, there was no significant change in body condition or body weight, as expected (Figure 3C), and no significant difference in testis-to-body weight ratio (Figure 3D), although assessments of testis weight alone did reveal a significant decline in the cKO (Figure S3G, $p < 0.05$). For a subset of observed animals, right and left testis weights were compared to identify any potential differences in phenotype severity, as reported previously;[18,29] however, no significant differences were found (Figure S3G), and all subsequent analyses were conducted via pooling of right and left testis cell populations. In performing quantitative measurements of sperm concentration in the cauda epididymis, a significant reduction was observed in EPAS1-cKO males ($p < 0.01$, Figure 3E), although no overt abnormalities were apparent in H&E-stained testis sections (Figure 3F). Assessments of testes from 12-month-old males uncovered equivalent results (Figures 3G–3I), with no significant difference in testis-to-body weight ratio (Figure 3G) or overt testis histology (Figure 3I); however, a significant decline in quantitative sperm output (Figure 3H, $p < 0.05$) was again identified between heterozygous and cKO males (an adverse event in the control cohort precluded the inclusion of these mice in the 12-month-old analyses). As with breeding data, comparisons of sperm production parameters at 2 and 12 months of age did not reveal any increase in severity of the phenotype with age (Figures S3H and S3I), as might be expected with an SSC self-renewal defect,[14] suggesting that EPAS1 expression is not absolutely required for SSC function in *steady-state* spermatogenesis.

Regardless, we performed quantitative analyses on germ cells at different stages of development in the testis to further confirm this (Figure S4). As expected, there was no significant reduction in the number of ZBTB16 (PLZF)+ undifferentiated spermatogonia per tubule (Figures S4A and S4B), nor the percentage of undifferentiated spermatogonia in mitosis (ZBTB16+/Ki67+) when comparing control and cKO testes (Figures S4A and S4C). In assessing the number of STRA8+ differentiating spermatogonia in seminiferous tubules at stage VII/VIII of the cycle of the seminiferous epithelium, there was again no significant difference between control and EPAS1-cKO testes (Figures S4D and S4E). Contrastingly, reduced germ cell abundance could be appreciated when quantifying numbers of elongated spermatids using a "daily sperm production" assay[30] ($p < 0.001$), accompanied by representative images in which round and elongated spermatids are stained with fluorescein isothiocyanate (FITC)-conjugated peanut agglutinin (PNA) lectin (Figures S4F and S4G). These data again suggest that SSC function is not significantly compromised in the EPAS1-cKO mouse in steady-state conditions, albeit modest impairments at the later stages of spermatogenesis are evident.

Finally, an assessment of viability and motility was performed on spermatozoa collected from the cauda epididymis. A small but significant reduction in viability was identified when comparing the spermatozoa of control and EPAS1-cKO males ($86\% \pm 4.2\%$ versus $70\% \pm 4.1\%$, $p < 0.05$, Figure 3J). This was accompanied by a reduction in total sperm motility that approached statistical significance ($53\% \pm 3.8\%$ versus $39\% \pm 4.7\%$, $p = 0.06$, Figure 3K), and a significant reduction in progressive motility ($36\% \pm 6.9\%$ versus $24\% \pm 5.5\%$, $p < 0.05$, Figure 3L).

EPAS1 expression is required for normal SSC function *in vivo* in regenerative conditions

Gene expression requirements for SSC function are known to be significantly altered in steady-state versus regenerative conditions.[19] Given that our earlier spermatogonial transplantation analyses (Figure 2H) suggested that modulation of EPAS1 expression significantly influences the regeneration of spermatogenesis by SSCs, and considering that HIFs have been identified as putative regulators of SSC regeneration post-chemotherapy treatment,[19] we next endeavored to explore the consequences of EPAS1 ablation on SSC function *in vivo* following low-dose busulfan treatment (Figure 4A). The busulfan treatment regimen was conducted in an equivalent manner to our previous studies[16]: treating control and EPAS1-cKO mice (~6 weeks of age) with a one-off intraperitoneal injection at 20 mg/kg (Figure 4A). Testes were collected at 14 days post-busulfan (Figure 4), a time point that has been previously defined to capture undifferentiated spermatogonia within their active period of regeneration,[19,31] and also at 12 weeks post-busulfan to assess long-term effects on spermatogenesis (Figure 5).

At 14 days post-busulfan treatment, a significant reduction in testis-to-body weight ratio was observed ($p < 0.01$, Figure 4B). This was accompanied by a significant reduction in the number of undifferentiated spermatogonia detected using an E-cadherin flow cytometry assay ($p < 0.05$, Figure 4C). A scRNA-seq analysis was performed on spermatogonia-enriched germ cell populations collected from control and EPAS1-cKO testes to extrapolate the mechanisms underlying this regeneration defect. Analyses of scRNA-seq results were conducted on a merged dataset (Butler et al., 2018) containing 1,033 control and 735 cKO germ cells. Unsupervized clustering projected onto uniform

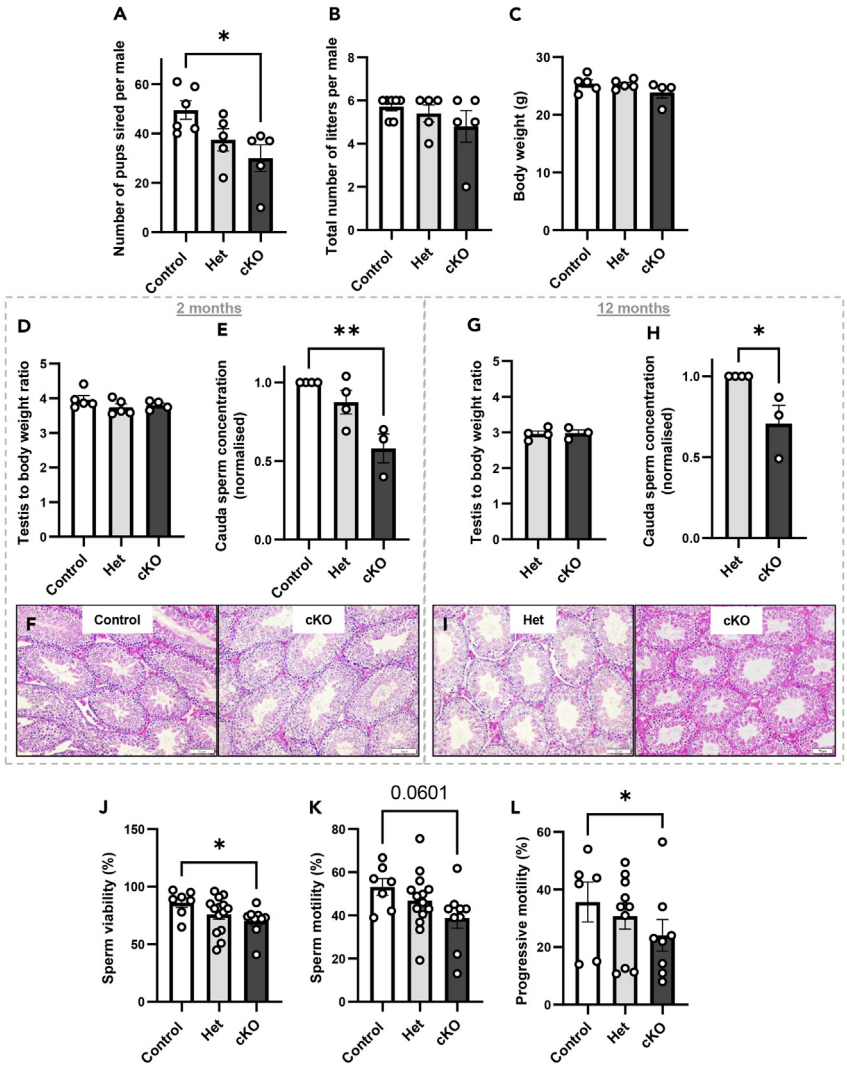

Figure 3. Exploring the effects of *Epas1* ablation in SSCs in steady-state conditions

(A) Number of pups sired per male over the duration of a breeding study. Control, heterozygous or EPAS1-cKO males were paired with control females up until 6 months of age. Histogram depicts mean ± SEM for n = 5–6 biological replicates, $p < 0.05$ (ANOVA). Additional breeding study data are provided in Figure S3.

(B) Total number of litters sired per male over the breeding study (n = 5–6).

(C) A comparison of body weight (grams) of control, heterozygous, and EPAS1-cKO mice at 2 months of age (n = 4–5).

(D) Testis-to-body weight ratio of control, heterozygous, and EPAS1-cKO mice at 2 months of age (n = 4–5). An accompanying left-versus-right testis weight comparison is provided in Figure S3G.

(E) Sperm concentration in the caudal region of the epididymis of control, heterozygous, and EPAS1-cKO mice at 2 months of age (n = 3–4, $p < 0.01$ (ANOVA)).

(F) Hematoxylin and eosin (H&E) stained testis sections from control and EPAS1-cKO mice at 2 months of age. Scale bar = 10μm.

(G) Testis-to-body weight ratio of heterozygous, and EPAS1-cKO mice at 12 months of age (n = 3–4).

(H) Epididymal sperm concentration of heterozygous and EPAS1-cKO mice at 12 months of age (n = 3–4, $p < 0.05$ (t test)).

(I) H&E stained testis sections from heterozygous and EPAS1-cKO mice at 12 months of age. Scale bar = 10μm.

(J) Viability of sperm collected from control, heterozygous, and EPAS1-cKO mice (n = 7–13, $p < 0.05$ (ANOVA)).

(K) Total motility of sperm collected from control, heterozygous, and EPAS1-cKO mice (n = 7–13, $p = 0.0601$ (ANOVA)).

(L) Progressive motility of sperm collected from control, heterozygous, and EPAS1-cKO mice (n = 6–10, $p < 0.05$ (ANOVA)).

manifold approximation and projection (UMAP) plots revealed 10 populations (Figure 4D) that could be broadly categorized as undifferentiated spermatogonia (clusters 0, 1, and 2; *Zbtb16*, *Etv5*, *Gfra1* expression), early-to-mid round spermatids (clusters 6, 7, and 8; *Acr*, *Acrv1*), mid-to-late round spermatids (clusters 3, 4, and 5, *Prm1*, *Gapdhs*), and one "undefined" cluster that contained only 18 cells (cluster 9, *Ly86*, *Cybb*) (Figures 4E, 4F, and S5A–S5D). Notably, no differentiating spermatogonia were captured, in line with the known dynamics of the spermatogonial pool at this time point in regeneration, in which the A to A1 transition has not yet resumed,[19,31] with spermatids captured here being a legacy of the cycle of spermatogenesis that preceded busulfan treatment. In assessing the number of cells associated with these

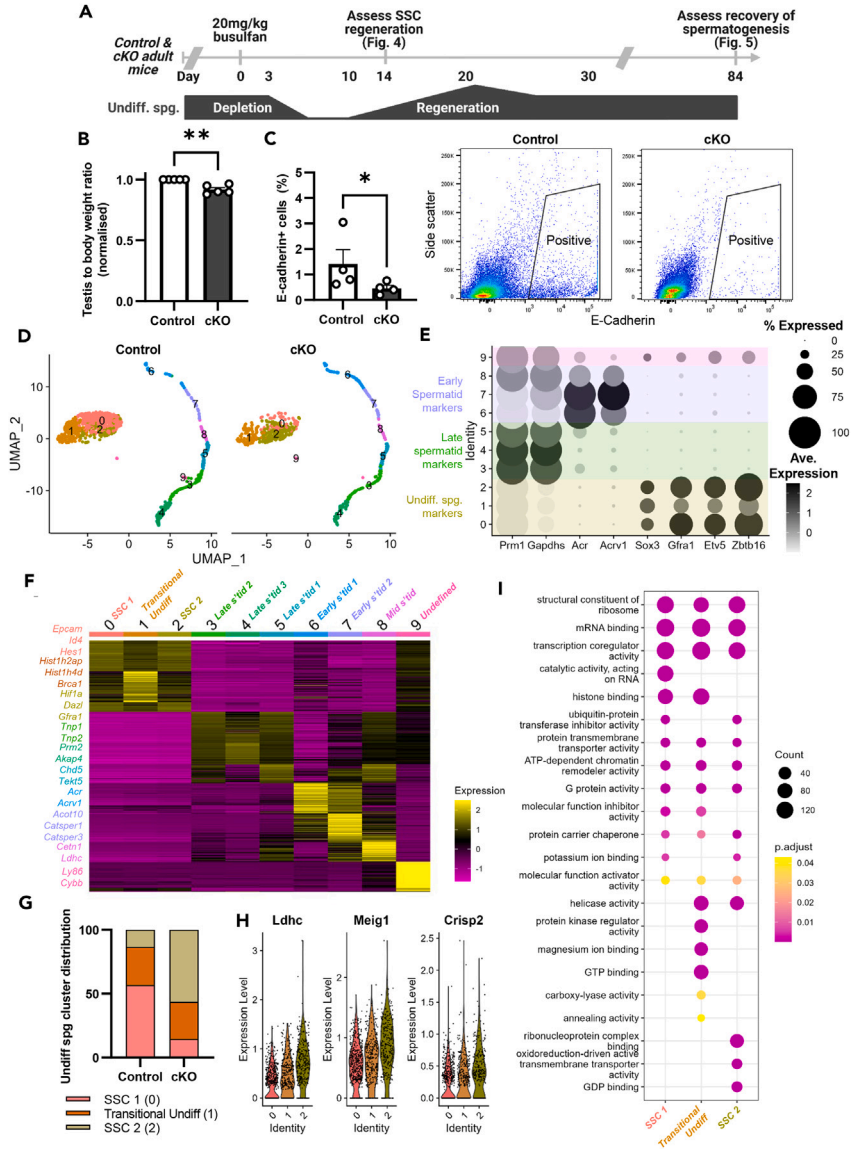

Figure 4. EPAS1 expression is required for normal SSC function in regenerative conditions

(A) (*Upper*) Timeline depicting the busulfan treatment regime used in this study. Assessments were carried out at 10 days (Figure 4) and 12 weeks (Figure 5) post-treatment. *(Lower)* Dynamics of the undifferentiated spermatogonia population following treatment with low-dose busulfan.

(B) Testis-to-body weight ratio for control and EPAS1-cKO males at 10 days post-busulfan treatment. Histogram depicts mean ± SEM (normalized) for n = 5 biological replicates. ** denotes significantly different at $p < 0.01$ (t test).

(C) (*Left*) Percentage of E-cadherin+ spermatogonia in control and cKO testes at 10 days post-busulfan treatment (n = 4, $p < 0.01$ (t test)). *(Right)* Representative flow cytometry images.

(D) UMAP plots depicting single cell RNA-seq analyses on germ cells from control and EPAS1-cKO testes at 10 days post-busulfan treatment.

(E) Dot plots depicting expression of known markers for undifferentiated spermatogonia, early and late spermatids in clusters 0–9. Dot size represents the percent of cells in each cluster exhibiting gene expression, dot color represents levels of expression.

(F) Heatmap depicting unique gene expression delineating clusters 0–9. Examples of unique markers for each cluster are listed on the left.

(G) Control and EPAS1-cKO undifferentiated spermatogonia show differential distribution between clusters. Control spermatogonia predominate cluster 0 ("SSC 1"), whereas cKO spermatogonia predominate cluster 2 ("SSC 2").

(H) Violin plots depicting the expression of a subset of genes that are significantly upregulated in cluster 2 ("SSC 2", cKO dominated cluster).

(I) GO analysis of unique cluster markers for clusters 0 ("SSC 1), 1 ("Transitional Undifferentiated") and 2 ("SSC 2"). Dot size corresponds to gene count for each biological process, dot color corresponds with adjusted p value.

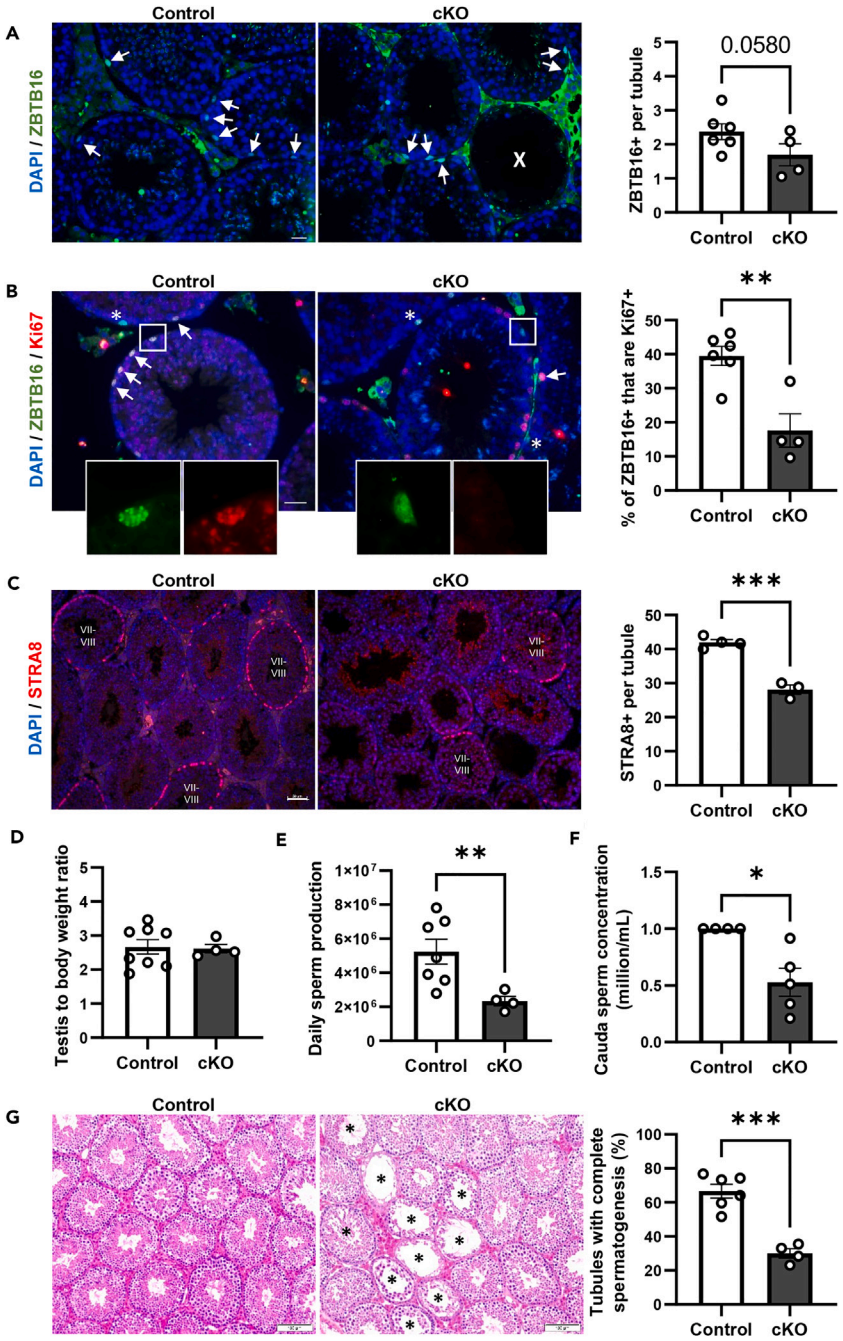

Figure 5. EPAS1 expression is required for normal recovery of spermatogenesis following busulfan treatment

(A) (*Left*) Immunofluorescence images depicting ZBTB16 (PLZF; green) expression in control and EPAS1-cKO testes at 12 weeks post-busulfan treatment. DAPI (blue) was used as a nuclear stain. White arrows depict ZBTB16+ spermatogonia. "X" depicts an empty tubule. Scale bar = 20 μm. *(Right)* Counts depicting the number of ZBTB16+ cells per tubule in control and EPAS1-cKO testes. Histogram depicts mean ± SEM for n = 4–6 biological replicates. p = 0.0580 (t test).

(B) (*Left*) Immunofluorescence images depicting ZBTB16 (green) and Ki67 (red) expression in control and EPAS1-cKO testes at 12 weeks post-busulfan treatment. White arrows depict ZBTB16+/Ki67+ cells, white asterisks depict ZBTB16+/Ki67- cells. Scale bar = 20 μm. *(Right)* Percentage of ZBTB16+ cells that are also Ki67+ (i.e., in mitosis) (n = 4–6, $p < 0.01$ (t test)).

(C) (*Left*) Immunofluorescence images depicting STRA8 (red) expression in control and EPAS1-cKO testes at 12 weeks post-busulfan treatment. DAPI (blue) was used as a nuclear stain. Scale bar = 50 μm. *(Right)* Counts depicting the number of STRA8+ cells per tubule (stage VII-VIII) in control and EPAS1-cKO testes (n = 3–4, $p < 0.001$ (t test)).

(D) Testis-to-body weight ratio for control and EPAS1-cKO mice at 12 weeks post-busulfan treatment (n = 4–8).

(E) Daily sperm production in control and EPAS1-cKO mice at 12 weeks post-busulfan treatment (n = 4–7, $p < 0.01$ (t test)).

Figure 5. *Continued*

(F) Concentration of sperm in the cauda epididymis, comparing control and EPAS1-cKO mice at 12 weeks post-busulfan treatment (n = 5, $p < 0.05$ (t test)).

(G) (*Left*) Representative images of H&E stained testis sections from control and EPAS1-cKO mice at 12 weeks post-busulfan treatment. Asterisks denote tubules with incomplete spermatogenesis. *(Right)* The percentage of tubules that displayed complete spermatogenesis at 12 weeks post-busulfan treatment (n = 4–6, $p < 0.001$ (t test)).

broader population identities, the number of spermatids captured from the control versus EPAS1-cKO testis was largely equivalent (331 for control versus 380 for cKO); however, the number of undifferentiated spermatogonia captured was reduced by ~30% in the EPAS1-cKO (1,033 in control versus 735 in cKO) (Figure S5B) in alignment with our initial E-cadherin flow cytometry analyses (Figure 4C) and further suggesting a regeneration impairment in SSCs. Within these broader cell identities, each cluster was delineated by unique marker expression (summarized in heatmap in Figure 4F and listed in Data S3) and unique enrichment of biological processes (GO analysis, Figures 4I and S5D).

In assessing the distribution of cells between clusters, distinct differences were apparent between genotypes ($p < 0.0001$, Figures 4D, 4G, and S5C). For undifferentiated spermatogonia (Figures 4G–4I), it could immediately be appreciated that EPAS1-cKO cells preferentially localized to different clusters than control spermatogonia (Figure 4D). For control undifferentiated spermatogonia, 57% were residing in cluster 0, 30% in cluster 1, and 13% in cluster 2 (Figure 4G). Contrastingly, for cKO spermatogonia, only 14% were residing in cluster 0, 29% in cluster 1, and 56% in cluster 2 (Figure 4G). In assigning identities to these clusters, we referred to the recently published scRNA-seq analyses of spermatogonial sub-populations in regenerative conditions to look for analogous marker expression.[19] Cluster 1, which was equivalently populated by both control and cKO cells, was identified to be in a "Transitional" undifferentiated state, with reduced expression of key stem cell genes such as *Gfra1* and *Etv5* (Figure 4E) and elevated expression of progenitor-associated genes such as *Sox3* (Figure 4E), alongside the expression of previously defined markers for "Transitional" regenerative spermatogonia, such as *Hist1h2ap*, *Hist1h4d*, and *Brca1*[19] (Figure 4F and Data S3). Cluster 0 and 2, which were primarily populated by either control or cKO spermatogonia, respectively, were identified as SSCs, exhibiting high levels of expression of *Id4*, *Gfra1*, *Etv5*, and *Lhx1* (Figures 4E and 4F; Data S3). In aligning cluster markers with the previously published regenerative SSC states, clusters 0 and 2 spanned transcriptional states that La et al. labeled as "Primitive" SSCs (*Etv5, Egr2, Dusp6*), and "Proliferative" SSCs (*Epcam, Hes1,* and *Ptgr1*) (Figure 4F and Data S3), perhaps a reflection of differences in the resolution of clustering and overall cell number between our studies. Regardless, in exploring changes in gene expression in the cKO-dominant SSC cluster (cluster 2) that could contribute to impaired SSC regeneration, multiple genes were significantly upregulated (*Crisp2*, *Meig1*, and *Ldhc*) (Figure 4H) that were hallmark genes of an "Undefined Undifferentiated" population of cells that La et al. (2022) found were not actively contributing to the SSC or progenitor populations using RNA velocity analyses.[19] Our own GO analyses also revealed alterations such as reduced histone binding in cluster 2 and increased oxidoreduction activity (Figure 4I). Additionally, in comparing differentially expressed genes (DEGs) of all control versus all cKO undifferentiated spermatogonia, GO analysis identified the enrichment of pathways previously identified in our Daprodustat bulk RNA-seq analysis (Figures 2I–2K, Data S2), including metabolism, processes associated with proteostasis, and cell cycle.

Finally, to establish whether these changes in gene expression and regeneration of SSCs in the EPAS1-cKO testis had long-term effects on spermatogenesis, we assessed testes at 12 weeks post-busulfan treatment (allowing for 2 rounds of spermatogenesis to ensue from exposed SSCs). Firstly, we determined that numbers of undifferentiated spermatogonia (ZBTB16+ cells per tubule) were lower in the cKO ($p = 0.0580$, Figure 5A), and the percentage of ZBTB16+ cells that were in mitosis (Ki67+) was significantly reduced ($p < 0.01$, Figure 5B), remaining at levels equivalent to that seen in steady-state conditions (Figure S4C). Contrastingly, proliferation in control undifferentiated spermatogonia in regenerative conditions was double that seen in steady state, again supporting the notion of a defective transition into "Proliferative SSC" or "Progenitor" states in the EPAS1-cKO. In cohesion with this, a significant reduction in the number of STRA8+ differentiating spermatogonia per tubule (stages VII-VIII) was also identified in the EPAS1-cKO (Figure 5C, $p < 0.001$). Although the testis-to-body weight ratio was largely restored at this time point (Figure 5D), daily sperm production ($p < 0.01$, Figure 5E) and epididymal sperm concentration ($p < 0.05$, Figure 5F) were significantly lower in the EPAS1-cKO, as was the number of tubules that had complete restoration of spermatogenesis ($p < 0.001$, Figure 5G). Overall, these analyses confirm that EPAS1 expression is important for the normal function of SSCs in regenerative conditions, including following exposure to chemotherapeutic reagents, and after spermatogonial transplantation.

DISCUSSION

Understanding a role for hypoxia and HIFs in regulating SSC function has important implications for understanding pathologies that affect male fertility, and for the development of treatment pipelines to reverse infertility. Here we have identified that SSCs reside in hypoxic niches in the testis and require expression of EPAS1 for normal SSC function, particularly in regenerative conditions such as following chemotherapy treatment. Additionally, we have provided insight into molecular pathways that are controlled by EPAS1 signaling in SSCs and have presented a novel methodology for improving SSC maintenance *in vitro* by modulating EPAS1 expression.

Our experiments using the oxygen-sensing probe pimonidazole and exploring HIF-alpha protein expression in SSCs and progenitors not only provided evidence for hypoxic SSC niches in the testis but also suggest that the transition into a progenitor state is accompanied by relocation into higher oxygen segments of the tubule. This finding has recently been supported by another research group that compared the broader spermatogonial populations of "undifferentiated" (CDH1+) and "differentiating" (KIT+) spermatogonia using pimonidazole/Hypoxyprobe, but similarly found that the differentiating spermatogonia had significantly lower percentages of Hypoxyprobe adduct formation.[26] Although the current manuscript has primarily focused on the mechanism by which hypoxia regulates the stem cell state, these findings infer the possibility that transition into higher oxygen environments and subsequent degradation of HIFs could release a "handbrake" that would otherwise prevent spermatogonial differentiation (as is the case in some other stem cell types[32]). In support of this theory, a recent study by Li and Yang[33] that

assessed germ cell populations in mice that had spent 4 weeks in a hypobaric hypoxic chamber demonstrated that, while SSC number remained unchanged (as assessed by spermatogonial transplantation), the overall number of undifferentiated spermatogonia (LIN28+) was reduced, suggesting an impairment in the SSC-to-progenitor transition. These findings are also potentially intertwined with previous studies where impairment of mitochondrial function in spermatogonia prevented the differentiating transition,[34] given that our RNA-seq analyses demonstrated increased expression of proteins involved in mitochondrial metabolism when EPAS1 was degraded.

In considering the association between EPAS1 signaling and improved SSC function in *in vitro* culture, this is also likely to be interconnected with the regulation of metabolism. Indeed, after only 24 h of Daprodustat treatment, we detected a significant increase in the expression of 19 genes associated with glycolysis. Such changes were accompanied by a 3-fold increase in colony formation after spermatogonial transplantation. These findings complement previous studies that have driven glycolytic metabolism to improve SSC maintenance *in vitro*, either by overexpression of *Myc*,[35] or by lowering O_2 concentration from 20% to 10%.[27] However, it is important to note that even in these glycolysis-promoting conditions, a stem cell decline was still evident over time.[27] We propose that this response is linked with continuing EPAS1 degradation under these non-hypoxic conditions (as demonstrated in Figures 2A and 2B), meaning that other downstream pathways (such as those highlighted in Figures 2J and 2K) that are normally active in SSCs *in vivo* become dysregulated. We also propose that our Daprodustat treatment regimen successfully improves SSC function by correcting this dysregulation via short-term treatment in the absence of feeder cells, while previous attempts to instigate hypoxic signaling in SSCs in culture were not successful because of detrimental impacts to the feeder cells resulting from long-term exposure to hypoxic conditions (cultured at 1%–5% O_2 on mouse embryonic fibroblast [MEF] feeder cells for 7 days).[26] These findings should be taken into consideration for the future optimization of SSC culture techniques, particularly in a clinical setting, as improved capacity for expansion of human SSCs *in vitro* could be a key component for the development of spermatogonial transplantation pipelines to reverse male infertility, particularly in survivors of pediatric cancers.[36]

An association between hypoxia (environmental and pathological) and reduced sperm output has long been appreciated; however, data produced from our EPAS1-cKO mouse model depict the requirement for a delicate balance of oxygen tension in the testis to ensure normal spermatogenesis. Patients and animal models that have pathological hypoxia (i.e., sleep apnea, sickle cell disease) and that are exposed to hypobaric hypoxia (i.e., high altitude) have been shown to have reduced sperm output and motility, which is largely restored when the hypoxic state is reversed (reviewed by Li et al.[37]). Based on our findings and those of others[33] we can hypothesize that this is because SSCs have adapted to reside in low-oxygen microenvironments and thus are not detrimentally affected. Rather, there is likely to be an impairment in the spermatogonial transition toward differentiation, which would reduce sperm output in pathological hypoxic conditions, but could "restart" robust sperm production when normal oxygen conditions are restored. On the other hand, our data suggest that hypoxic microenvironments and HIF signaling are involved in regulating the normal function of SSCs in the testis, with EPAS1 ablation in germ cells also resulting in reduced sperm output, motility, and viability, accompanied by a modest reduction in fertility (Figure 3). Although beyond the scope of this study, one could speculate that the detriment to functional parameters of mature sperm could be linked with mitochondrial abnormalities and oxidative stress acquired at the earlier stages of germ cell development, given that these were common pathologies in other cell types in the *Epas1* global knockout mouse line.[11] Beyond this, we have demonstrated that EPAS1 signaling is required for the normal regeneration of spermatogenesis by SSCs following either transplantation or chemotherapy treatment (Figures 4 and 5). Thus, in looking at this through the lens of human fertility, any dysregulation to the EPAS1 signaling pathway, through either genetic mutation[38] or the administration of EPAS1-targeting medications (such as Belzutifan[39]), could be highly problematic for male fertility, particularly when SSCs are diverted into a regenerative state. Again, a delicate balance of hypoxia and HIF signaling seems to be required for optimal male fertility.

In conclusion, this study has generated a novel EPAS1-cKO mouse line and transcriptomic databases (both RNA-seq and scRNA-seq) to improve our understanding of the role of hypoxia and HIF signaling pathways in SSCs. We have concluded that, as is the case for a number of other stem cell types, SSCs reside in hypoxic microenvironments in the testis, while the transition to a progenitor state is accompanied by a shift toward higher-oxygen segments of the seminiferous tubule. The expression of EPAS1 was shown to be important for robust SSC function, both in *in vitro* culture and in the testis, particularly following chemotherapeutic exposure. These findings make an important contribution to our understanding of the relationship between male fertility/infertility and hypoxia, and how this relates to SSC function.

Limitations of the study

Although this study demonstrates that SSCs reside in hypoxic environments in the testis and show phenotypic differences following germline ablation of the hypoxia-inducible factor *Epas1*, equivalent experiments have not yet been performed for *Hif1a*, which is also expressed within the SSC population. Given that EPAS1 and HIF1A are known to share a subset of target genes (in addition to a suite of individual unique gene targets), in future studies it would be informative to create an *Epas1*/*Hif1a* double-germline knockout to uncover the full extent of hypoxia-driven pathways in regulating SSC function.

STAR★METHODS

Detailed methods are provided in the online version of this paper and include the following:

- KEY RESOURCES TABLE
- RESOURCE AVAILABILITY
  - Lead contact
  - Materials availability

SUPPLEMENTAL INFORMATION

Supplemental information can be found online at https://doi.org/10.1016/j.isci.2023.108424.

ACKNOWLEDGMENTS

This research was supported by grant APP1181024 awarded to T.L. and B.N. from the National Health and Medical Research Council of Australia, the Bob and Terry Kennedy Infertility Grant awarded to T.L. from the Hunter Medical Research Institute, and a Discovery Early Career Research Award (DE220100032) awarded to T.L. by the Australian Research Council. B.N. is the recipient of a National Health and Medical Research Council of Australia Senior Research Fellowship (APP1154837).

Thank you to Nicole Cole from the University of Newcastle's Central Analytical facilities for her assistance with FACS isolations. Thank you to the HMRI Core Histology Facility for their assistance in tissue processing, sectioning, and staining.

AUTHOR CONTRIBUTIONS

Conceptualization: T.L., Investigation: I.R.B., B.N., J.M.L., K.B.D., C.S.D.O., N.S.M., S.J.S., G.E.K., T.H.Y., J.M.O., N.M.S., J.L.P., and T.L., Writing – Original Draft: T.L., Writing – Review and Editing: T.L. and B.N., Funding Acquisition: T.L. and B.N.

DECLARATION OF INTERESTS

The authors have no competing interests to declare.

Received: August 10, 2023
Revised: September 21, 2023
Accepted: November 7, 2023
Published: November 9, 2023

REFERENCES

1. Jež, M., Rožman, P., Ivanović, Z., and Bas, T. (2015). Concise Review: The Role of Oxygen in Hematopoietic. Stem Cell Physiol. *230*, 1999–2005.
2. Lord, T., and Nixon, B. (2020). Metabolic changes accompanying spermatogonial stem cell differentiation. Dev. Cell *52*, 399–411.
3. Ivan, M., Kondo, K., Yang, H., Kim, W., Valiando, J., Ohh, M., Salic, A., Asara, J.M., Lane, W.S., and Kaelin, W.G., Jr. (2001). HIFalpha targeted for VHL-mediated destruction by proline hydroxylation: implications for O2 sensing. Science *292*, 464–468.
4. Jaakkola, P., Mole, D.R., Tian, Y.M., Wilson, M.I., Gielbert, J., Gaskell, S.J., von Kriegsheim, A., Hebestreit, H.F., Mukherji, M., Schofield, C.J., et al. (2001). Targeting of HIF-alpha to the von Hippel-Lindau ubiquitylation complex by O2-regulated prolyl hydroxylation. Science *292*, 468–472.
5. Yu, F., White, S.B., Zhao, Q., and Lee, F.S. (2001). HIF-1alpha binding to VHL is regulated by stimulus-sensitive proline hydroxylation. Proc. Natl. Acad. Sci. USA *98*, 9630–9635.
6. Semenza, G.L. (1999). Regulation of Mammalian O2 Homeostasis by Hypoxia-Inducible Factor 1. Annu. Rev. Cell Dev. Biol. *15*, 551–578.
7. Keith, B., Johnson, R.S., and Simon, M.C. (2011). HIF1α and HIF2α: sibling rivalry in hypoxic tumour growth and progression. Nat. Rev. Cancer *12*, 9–22.
8. Dengler, V.L., Galbraith, M., and Espinosa, J.M. (2014). Transcriptional regulation by hypoxia inducible factors. Crit. Rev. Biochem. Mol. Biol. *49*, 1–15.
9. Oatley, J.M., and Brinster, R.L. (2012). THE GERMLINE STEM CELL NICHE UNIT IN MAMMALIAN TESTES. Physiol. Rev. *92*, 577–595.
10. Rebourcet, D., Wu, J., Cruickshanks, L., Smith, S.E., Milne, L., Fernando, A., Wallace, R.J., Gray, C.D., Hadoke, P.W.F., Mitchell, R.T., et al. (2016). Sertoli Cells Modulate Testicular Vascular Network Development, Structure, and Function to Influence Circulating Testosterone Concentrations in Adult Male Mice. Endocrinology *157*, 2479–2488.
11. Scortegagna, M., Ding, K., Oktay, Y., Gaur, A., Thurmond, F., Yan, L.J., Marck, B.T., Matsumoto, A.M., Shelton, J.M., Richardson, J.A., et al. (2003). Multiple organ pathology, metabolic abnormalities and impaired homeostasis of reactive oxygen species in Epas1-/- mice. Nat. Genet. *35*, 331–340.

12. Gruber, M., Mathew, L.K., Runge, A.C., Garcia, J.A., and Simon, M.C. (2010). EPAS1 Is Required for Spermatogenesis in the Postnatal Mouse Testis. Biol. Reprod. *82*, 1227–1236.
13. Gruber, M., Hu, C.-J., Johnson, R.S., Brown, E.J., Keith, B., and Simon, M.C. (2007). Acute postnatal ablation of Hif-2α results in anemia. Proc. Natl. Acad. Sci. USA *104*, 2301–2306.
14. Oatley, M.J., Kaucher, A.V., Racicot, K.E., and Oatley, J.M. (2011). Inhibitor of DNA Binding 4 Is Expressed Selectively by Single Spermatogonia in the Male Germline and Regulates the Self-Renewal of Spermatogonial Stem Cells in Mice. Biol. Reprod. *85*, 347–356.
15. Iyer, N.V., Kotch, L.E., Agani, F., Leung, S.W., Laughner, E., Wenger, R.H., Gassmann, M., Gearhart, J.D., Lawler, A.M., Yu, A.Y., and Semenza, G.L. (1998). Cellular and developmental control of O2 homeostasis by hypoxia-inducible factor 1 alpha. Genes Dev. *12*, 149–162.
16. Lord, T., Law, N.C., Oatley, M.J., Miao, D., Du, G., and Oatley, J.M. (2022). A novel high throughput screen to identify candidate molecular networks that regulate spermatogenic stem cell functions. Biol. Reprod. *106*, 1175–1190.
17. Helsel, A.R., Yang, Q.-E., Oatley, M.J., Lord, T., Sablitzky, F., and Oatley, J.M. (2017). ID4 levels dictate the stem cell state in mouse spermatogonia. Development *144*, 624–634.
18. Bustamante-Marin, X.M., Cook, M.S., Gooding, J., Newgard, C., and Capel, B. (2015). Left-Biased Spermatogenic Failure in 129/SvJ Dnd1Ter/+ Mice Correlates with Differences in Vascular Architecture, Oxygen Availability, and Metabolites. Biol. Reprod. *93*, 78.
19. La, H.M., Liao, J., Legrand, J.M.D., Rossello, F.J., Chan, A.-L., Vaghjiani, V., Cain, J.E., Papa, A., Lee, T.L., and Hobbs, R.M. (2022). Distinctive molecular features of regenerative stem cells in the damaged male germline. Nat. Commun. *13*, 2500.
20. Chan, F., Oatley, M.J., Kaucher, A.V., Yang, Q.-E., Bieberich, C.J., Shashikant, C.S., and Oatley, J.M. (2014). Functional and molecular features of the Id4+ germline stem cell population in mouse testes. Genes Dev. *28*, 1351–1362.
21. Law, N.C., Oatley, M.J., and Oatley, J.M. (2019). Developmental kinetics and transcriptome dynamics of stem cell specification in the spermatogenic lineage. Nat. Commun. *10*, 2787.
22. Hermann, B.P., Cheng, K., Singh, A., Roa-De La Cruz, L., Mutoji, K.N., Chen, I.C., Gildersleeve, H., Lehle, J.D., Mayo, M., Westernströer, B., et al. (2018). The Mammalian Spermatogenesis Single-Cell Transcriptome, from Spermatogonial Stem Cells to Spermatids. Cell Rep. *25*, 1650–1667.e8.
23. Guo, J., Grow, E.J., Mlcochova, H., Maher, G.J., Lindskog, C., Nie, X., Guo, Y., Takei, Y., Yun, J., Cai, L., et al. (2018). The adult human testis transcriptional cell atlas. Cell Res. *28*, 1141–1157.
24. Guo, J., Nie, X., Giebler, M., Mlcochova, H., Wang, Y., Grow, E.J., DonorConnect, Kim, R., Tharmalingam, M., Matilionyte, G., et al. (2020). The Dynamic Transcriptional Cell Atlas of Testis Development during Human Puberty. Cell Stem Cell *26*, 262–276.e4.
25. Varia, M.A., Calkins-Adams, D.P., Rinker, L.H., Kennedy, A.S., Novotny, D.B., Fowler, W.C., Jr., and Raleigh, J.A. (1998). Pimonidazole: a novel hypoxia marker for complementary study of tumor hypoxia and cell proliferation in cervical carcinoma. Gynecol. Oncol. *71*, 270–277.
26. Morimoto, H., Yamamoto, T., Miyazaki, T., Ogonuki, N., Ogura, A., Tanaka, T., Kanatsu-Shinohara, M., Yabe-Nishimura, C., Zhang, H., Pommier, Y., et al. (2021). An interplay of NOX1-derived ROS and oxygen determines the spermatogonial stem cell self-renewal efficiency under hypoxia. Genes Dev. *35*, 250–260.
27. Helsel, A.R., Oatley, M.J., and Oatley, J.M. (2017). Glycolysis-Optimized Conditions Enhance Maintenance of Regenerative Integrity in Mouse Spermatogonial Stem Cells during Long-Term Culture. Stem Cell Rep. *8*, 1430–1441.
28. Gallardo, T., Shirley, L., John, G.B., and Castrillon, D.H. (2007). Generation of a germ cell-specific mouse transgenic Cre line. Vasa-Cre. Genesis *45*, 413–417.
29. Bustamante-Marin, X.M., and Capel, B. (2023). Oxygen availability influences the incidence of testicular teratoma in Dnd1Ter/+ mice. Front. Genet. *14*, 1179256.
30. Cotton, L., Gibbs, G.M., Sanchez-Partida, L.G., Morrison, J.R., de Kretser, D.M., and O'Bryan, M.K. (2006). FGFR-1 signaling is involved in spermiogenesis and sperm capacitation. J. Cell Sci. *119*, 75–84.
31. van Keulen, C.J., and de Rooij, D.G. (1974). The recovery from various gradations of cell loss in the mouse seminiferous epithelium and its implications for the spermatogonial stem cell renewal theory. Cell Tissue Kinet. *7*, 549–558.
32. Cui, P., Zhang, P., Yuan, L., Wang, L., Guo, X., Cui, G., Zhang, Y., Li, M., Zhang, X., Li, X., et al. (2021). HIF-1α Affects the Neural Stem Cell Differentiation of Human Induced Pluripotent Stem Cells via MFN2-Mediated Wnt/β-Catenin Signaling. Front. Cell Dev. Biol. *9*, 671704.
33. Li, S., and Yang, Q.-E. (2022). Hypobaric hypoxia exposure alters transcriptome in mouse testis and impairs spermatogenesis in offspring. Gene *823*, 146390.
34. Varuzhanyan, G., Rojansky, R., Sweredoski, M.J., Graham, R.L.J., Hess, S., Ladinsky, M.S., and Chan, D.C. (2019). Mitochondrial fusion is required for spermatogonial differentiation and meiosis. Elife *8*, e51601.
35. Kanatsu-Shinohara, M., Tanaka, T., Ogonuki, N., Ogura, A., Morimoto, H., Cheng, P.F., Eisenman, R.N., Trumpp, A., and Shinohara, T. (2016). Myc/Mycn-mediated glycolysis enhances mouse spermatogonial stem cell self-renewal. Genes Dev. *30*, 2637–2648.
36. Gassei, K., and Orwig, K.E. (2016). Experimental methods to preserve male fertility and treat male factor infertility. Fertil. Steril. *105*, 256–266.
37. Li, Z., Wang, S., Gong, C., Hu, Y., Liu, J., Wang, W., Chen, Y., Liao, Q., He, B., Huang, Y., et al. (2021). Effects of Environmental and Pathological Hypoxia on Male Fertility. Front. Cell Dev. Biol. *9*, 725933.
38. Lappin, T.R., and Lee, F.S. (2019). Update on mutations in the HIF: EPO pathway and their role in erythrocytosis. Blood Rev. *37*, 100590.
39. Zhou, J., and Gong, K. (2022). Belzutifan: a novel therapy for von Hippel–Lindau disease. Nat. Rev. Nephrol. *18*, 205–206.
40. Oatley, J.M., and Brinster, R.L. (2006). Spermatogonial Stem Cells. In Methods in Enzymology, K. Irina and L. Robert, eds. (Academic Press), pp. 259–282.
41. Nixon, B., Anderson, A.L., Bromfield, E.G., Martin, J.H., Lord, T., Cafe, S.L., Roman, S.D., Skerrett-Byrne, D.A., Eamens, A.L., De Iuliis, G.N., and Johnston, S.D. (2021). Gross and microanatomy of the male reproductive duct system of the saltwater crocodile Crocodylus porosus. Reprod. Fertil. Dev. *33*, 540–554.
42. Nakata, H., Wakayama, T., Takai, Y., and Iseki, S. (2015). Quantitative analysis of the cellular composition in seminiferous tubules in normal and genetically modified infertile mice. J. Histochem. Cytochem. *63*, 99–113.
43. Lord, T., Martin, J.H., and Aitken, R.J. (2015). Accumulation of electrophilic aldehydes during post-ovulatory ageing of mouse oocytes causes reduced fertility, oxidative stress and apoptosis. Biol. Reprod. *92*, 1–13.
44. Brinster, R.L., and Avarbock, M.R. (1994). Germline transmission of donor haplotype following spermatogonial transplantation. Proc. Natl. Acad. Sci. USA *91*, 11303–11307.
45. Brinster, R.L., and Zimmermann, J.W. (1994). Spermatogenesis following male germ-cell transplantation. Proc. Natl. Acad. Sci. USA *91*, 11298–11302.
46. Helsel, A.R., and Oatley, J.M. (2017). Transplantation as a Quantitative Assay to Study Mammalian Male Germline Stem Cells. In Germline Stem Cells, M. Buszczak, ed. (Springer New York), pp. 155–172.
47. Trigg, N.A., Skerrett-Byrne, D.A., Xavier, M.J., Zhou, W., Anderson, A.L., Stanger, S.J., Katen, A.L., De Iuliis, G.N., Dun, M.D., Roman, S.D., et al. (2021). Acrylamide modulates the mouse epididymal proteome to drive alterations in the sperm small non-coding RNA profile and dysregulate embryo development. Cell Rep. *37*, 109787.
48. Biggers, J.D., Whitten, W.K., and Whittingham, D.G. (1971). The Culture of Mouse Embryos in Vitro (W. H. Freeman).
49. Smith, T.B., Baker, M.A., Connaughton, H.S., Habenicht, U., and Aitken, R.J. (2013). Functional deletion of Txndc2 and Txndc3 increases the susceptibility of spermatozoa to age-related oxidative stress. Free Radic. Biol. Med. *65*, 872–881.
50. Huang, D.W., Sherman, B.T., and Lempicki, R.A. (2009). Systematic and integrative analysis of large gene lists using DAVID bioinformatics resources. Nat. Protoc. *4*, 44–57. https://www.nature.com/articles/nprot.2008.211#supplementary-information.
51. Huang, D.W., Sherman, B.T., and Lempicki, R.A. (2009). Bioinformatics enrichment tools: paths toward the comprehensive functional analysis of large gene lists. Nucleic Acids Res. *37*, 1–13.
52. Butler, A., Hoffman, P., Smibert, P., Papalexi, E., and Satija, R. (2018). Integrating single-cell transcriptomic data across different conditions, technologies, and species. Nat. Biotechnol. *36*, 411–420.
53. Wu, T., Hu, E., Xu, S., Chen, M., Guo, P., Dai, Z., Feng, T., Zhou, L., Tang, W., Zhan, L., et al. (2021). clusterProfiler 4.0: A universal enrichment tool for interpreting omics data. Innovation *2*, 100141.
54. Yu, G., Wang, L.G., Han, Y., and He, Q.Y. (2012). clusterProfiler: an R package for comparing biological themes among gene clusters. OMICS *16*, 284–287.

STAR★METHODS

KEY RESOURCES TABLE

REAGENT or RESOURCE	SOURCE	IDENTIFIER
Antibodies		
Rabbit pAb to EPAS1	Novus Biologicals	NB100-122; RRID: AB_10002593
Rabbit pAb to HIF1A	Invitrogen	PA1-16601; RRID: AB_2117128
Goat pAb to GFP	Abcam	ab6673; RRID: AB_305643
Mouse mAb to alpha-Tubulin	Sigma Aldrich	T5168; RRID: AB_477579
Rabbit pAb to pimonidazole	Hypoxyprobe	PAb2627AP; RRID: AB_2811309
Mouse mAb to PLZF	Santa Cruz	sc-28319; RRID: AB_2218941
Rabbit pAB to Ki67	Abcam	ab15580; RRID: AB_443209
Rabbit pAB to STRA8	Abcam	ab49405; RRID: AB_945677
Mouse mAB to SALL4	Abcam	ab57577; RRID: AB_2183366
Rat mAB to E-Cadherin, APC-conjugated	Biolegend	#147311; RRID: AB_2750300
Rat mAB to CD49f, Biotin-conjugated	Miltenyi	130-097-243; RRID: AB_2658557
Anti-Biotin microbeads	Miltenyi	130-090-485; RRID: AB_244365
Deposited data		
RNA-seq data (control versus Daprodustat treated spermatogonia)	GEO database	GSE235319 (GSE235531 Super series)
scRNA-seq data (control versus EPAS1-cKO germ cells)	GEO database	GSE235453 (GSE235531 Super series)
Previously published scRNA-seq data (postnatal day 6 mouse testis, published by Law et al.[21])	GEO database	GSE124904
Experimental models: Organisms/strains		
Mouse: *Id4-eGfp*: *Id4-eGfp* hemizygous	A gift from Professor Jon M. Oatley at Washington State University[20]	N/A
Mouse: *Rosa26-LacZ*: *Rosa26-LacZ* homozygous	Jackson Laboratories	112073
Mouse: *Ddx4* (*Vasa*)-Cre: *Ddx4* (*Vasa*)-Cre heterozygous	Jackson Laboratories	006954
Mouse: *Epas1*-loxP: *Epas1*-loxP homozygous	Jackson Laboratories	008407
Oligonucleotides		
Ddx4-Cre genotyping primers	ThermoFisher Scientific	Internal positive control: Fwd: 5′ CTA GGC CAC AGA ATT GAA AGA TCT 3′ Rev: 5′ GTA GGT GGA AAT TCT AGC ATC ATC C 3′ Transgene: Fwd: 5′ CAC GTG CAG CCG TTT AAG CCG CGT 3′ Rev: 5′ TTC CCA TTC TAA ACA ACA CCC TGA A 3′
Epas1-fl genotyping primers	ThermoFisher Scientific	Fwd: 5′ CAG GCA GTA TGC CTG GCT AAT TCC AGT T 3′ Rev 1: 5′ CTT CTT CCA TCA TCT GGG ATC TGG GAC T 3′ Rev 2: 5′ GCT AAC ACT GTA CTG TCT GAA AGA GTA GC 3′
Software and algorithms		
GraphPad Prism	GraphPad	v9.5.1

RESOURCE AVAILABILITY

Lead contact

Further information and requests for resources and reagents should be directed to and will be fulfilled by the lead contact, Dr Tessa Lord (Tessa.lord@newcastle.edu.au).

Materials availability

This study did not generate new unique reagents.

Data and code availability

- Data: Transcriptome (RNA-seq and scRNA-seq) data generated and analyzed in this study are available from the GEO database (accession number GSE235531). Previously published scRNA-seq databases that were accessed and mined for this study are as follows, PD6 mouse spermatogonia: GSE124904.[21]
- Code: This paper does not report original code.
- Any additional information required to reanalyse the data reported in this paper is available from the lead contact upon request.

EXPERIMENTAL MODEL AND STUDY PARTICIPANT DETAILS

Animal studies

All procedures involving animal use were approved by the University of Newcastle Animal Care and Ethics Committee (ACEC, approval number A-2019-907). The *Id4-eGfp* mouse line[20] was a gift from Dr Jon Oatley, and also carried the *Rosa26-LacZ* transgene (Jackson Laboratories, stock number 112073) to provide a donor cell population for spermatogonial transplantation experiments (P6-8 and adult (>6 weeks) male mice). C57BL/6 × CBA F1 males were used as recipients for spermatogonial transplantation (produced by the University of Newcastle Animal Services Unit (ASU)). Recipients were pre-treated with 45 mg/kg busulfan at 5–8 weeks of age (Sigma Aldrich, MO, USA) to ablate endogenous spermatogenesis, as described previously.[40]

Ddx4 (*Vasa*)-Cre[28] and *Epas1*-loxP[13] mouse lines were obtained from Jackson Laboratories (stock numbers 006954 and 008407, respectively). *Ddx4*-Cre, *Epas1*$^{-/+}$ males (5–10 weeks of age) were bred with *Epas1*$^{fl/fl}$ females to generate conditional knockout (cKO) animals (*Ddx4*-Cre, *Epas1*$^{fl/-}$) and control littermates. Primer sequences used for genotyping have been provided in Table S1. To instigate regenerative conditions in the testes of EPAS1-cKO males and accompanying controls, mice were treated with a one-off intraperitoneal injection of busulfan (20 mg/kg), in alignment with previously described protocols.[16,19]

Primary cultures of undifferentiated spermatogonia

Primary cultures were established from the ID4-eGFP+ population of undifferentiated spermatogonia from PD6-8 mouse testes and were maintained as described previously.[16] Briefly, cultures were maintained in 10% O_2, 5% CO_2 at 37°C mouse serum-fee medium (mSFM) supplemented with the growth factors GDNF (20 ng/mL; R&D systems, MN, USA) and fibroblast growth factor (FGF2) (1 ng/mL; Sigma Aldrich). Cultures were seeded on a feeder layer of mitotically inactivated SNL76/7 mouse embryonic fibroblasts (ATCC, VA, USA). Cells were passaged every 6–8 days onto fresh feeders, and media was replaced every second day.

For experiments where undifferentiated spermatogonia in culture were treated with the prolyl-hydroxylase inhibitor Daprodustat (250 μM; MedChemExpress, NJ, USA), spermatogonia were dislodged from the feeder layer using gentle pipetting. Isolated spermatogonia were then treated with Daprodustat or vehicle (DMSO) overnight (24 h) in mSFM plus growth factors. Spermatogonia were then washed in mSFM, before continuing with experimentation (i.e., flow cytometry, spermatogonial transplantation, or RNA-seq).

METHODS DETAILS

Flow cytometric analysis and cell sorting

Fluorescence-activated cell sorting (FACS) of ID4-eGFP^{Bright} and ID4-eGFP^{Dim} populations of spermatogonia from PD6-8 testes was conducted using a BD FACS AriaIIu using previously described gating parameters (Helsel et al.,[17]; Figure 1C). For flow cytometric assessment of cell viability and ID4-eGFP populations in primary cultures of spermatogonia, cells were loaded with a LIVE/DEAD Fixable Far Red Dead Cell Stain (ThermoFisher Scientific, MA, USA) and analyzed on a BD FACS Canto IIA machine using parameters described previously.[16]

To assess numbers of undifferentiated spermatogonia in control and EPAS1-cKO testes at 14 days post-busulfan treatment, an APC-conjugated E-Cadherin antibody (Biolegend, CA, USA; #147311, Table S2) was utilised, as per previously published methodologies.[19] Briefly, a single cell suspension was generated via a 5 min incubation in Collagenase IA at 37°C (Sigma Aldrich), followed by a 5 min 37°C incubation with pipetting in 0.25% Trypsin-EDTA containing 7mg DNase I (Sigma Aldrich). From herein, the single cell suspension was kept on ice in Phosphate Buffered Saline (PBS, Sigma Aldrich) containing 10% Fetal Bovine Serum (FBS, Cell Sera Australia, NSW, Australia). The anti-E-Cadherin antibody was used at a 1:250 dilution (Table S2) and incubated with cells for 30 min on ice. Cells were washed once in PBS/FBS solution before assessment on the flow cytometer.

Hypoxyprobe analyses

A Hypoxyprobe Omni Kit was utilised as per the manufacturer's instructions (Hypoxyprobe, MA, USA) to perform an *in situ* assessment of oxygen concentration experienced by SSCs and progenitor spermatogonia in the testis. Specifically, adult and PD6 mice were dosed with 60 mg/kg pimonidazole via intraperitoneal injection. Thirty minutes later, mice were culled and testes were collected for fixation or trypsin digestion to create a single cell suspension from which *Id4-Gfp* spermatogonia were isolated. To generate a positive control, testes were incubated with pimonidazole in 5% O_2 for 2 h before fixation. In order to detect pimonidazole adducts, an anti-Hypoxyprobe antibody was used (Table S2), following procedures described below for immunofluorescence staining and immunoblotting analysis. Given that Hypoxyprobe generates diffuse staining throughout the testis (Figure S1H), only cells with bright Hypoxyprobe fluorescence (white arrows in Figures 1E and 1F) were counted as having a positive signal.

Immunofluorescence staining

For immunofluorescence analysis on testis sections, adult or PD6 mouse testes were fixed in 4% paraformaldehyde (Sigma Aldrich) or Bouins solution (Sigma Aldrich) and embedded in paraffin. Sections were cut at 5 μm thickness and placed on microscope slides. Slides were moved through a series of xylene and ethanol washes (100%, 75% and 50% ethanol in H_2O) to achieve dewaxing and rehydration, respectively. Antigen retrieval was conducted via a 10 min incubation in boiling 10 mM sodium citrate buffer (pH 6). Prior to antibody incubations, sections were blocked in 3% Bovine Serum Albumin (BSA; Sigma Aldrich) in PBS and 10% goat serum (Sigma Aldrich) for 1 h. Primary antibodies and the concentrations at which they were utilised are listed in Table S2. Incubation in primary antibody was conducted overnight at 4°C. Sections were then washed three times in 1% BSA/PBS before administration of secondary antibodies (Alexa Fluor 488 and 594; ThermoFisher) for 1 h at room temperature at a concentration of 1/1000 in 1% BSA/PBS. For slides counterstained with FITC-conjugated PNA lectin (Sigma Aldrich, #L7381), sections were incubated with 5 μg/mL PNA for 20 min at 37°C, as described previously.[41] Staging of spermatogenesis was conducted based on PNA staining patterns previously depicted in Nakata et al.[42] Finally, all slides were counterstained with the nuclear stain DAPI (1/1000, Sigma Aldrich)), mounted in Mowiol containing 1,4-diazabicyclo[2.2.2]octane (DABCO) (Sigma Aldrich) and imaged on Zeiss Axio A.2 fluorescence microscope (Carl Zeiss Micro Imaging GmbH, Jena, Thuringia, Germany). For analyses where the percentage of positively stained cells was quantified, cells within at least 50 tubules per replicate were counted, with up to 100 tubules being counted for rare cell populations. Where the number of positively stained cells per tubule was calculated, elongated tubules (i.e., those not cut in transverse) were excluded.

For immunocytochemistry analyses, cells were fixed in 4% paraformaldehyde for 30 min and settled on poly-L-lysine coated coverslips. Cells were permeabilised in 0.2% Triton X-(Sigma Aldrich) in PBS for 10 min at room temperature, then blocked for 1 h in 10% goat serum in 3% BSA/PBS. Primary antibodies were used at concentrations denoted in Table S2, and incubated with cells overnight at 4°C. After three washes in 1% BSA/PBS, cells were incubated in secondary antibody (Alexa Fluor 488 and 594) at a concentration of 1/1000 for 1 h at room temperature. Coverslips were mounted on slides using Mowiol and were imaged on a Zeiss Axio A.2 fluorescence microscope or an FV1000 confocal microscope (Olympus, Tokyo, Japan). For analysis of corrected total cell fluorescence (CTCF), the public sector image-processing program ImageJ was utilised (version 1.53k; National Institutes of Health).

SDS-PAGE and Western blot analysis

Procedures for SDS-PAGE and Western blotting were performed as described previously,[43] however will be briefly recounted here. Protein extraction was achieved via a 5 min incubation at 100°C in SDS extraction buffer (2% [w/v] SDS and 10% [w/v] sucrose in 0.1875 M Tris, pH 6.8) containing protease inhibitor cocktail (Roche, Basel, Switzerland). Protein lysates were resolved on a 4–20% precast polyacrylamide gel (BioRad, CA, USA), prior to Western transfer onto nitrocellulose membrane using standard techniques. Membranes were subjected to a 1 h blocking step, using 5% skim milk diluted in Tris-Buffered Saline with 0.1% Tween (TBST). Incubation in primary antibody was conducted overnight at 4°C, and antibody concentrations used can be found in Table S2. Membranes were then washed three times TBST before a 1 h incubation in secondary antibody (goat anti-rabbit or goat anti-mouse IgG HRP). Signal was developed using ECL prime chemiluminescence detection reagent (GE Healthcare, IL, USA) and blots were visualised on a LAS4000 imager (GE Healthcare). Densitometry was performed using ImageJ, and values were normalised to the loading control (alpha-tubulin).

Spermatogonial transplantation

Spermatogonial transplantation was conducted using methods described previously[44–46] to compare SSC numbers in undifferentiated cultures of spermatogonia treated with Daprodustat (i.e., with increased stability of EPAS1) versus control (DMSO treated) cells. Approximately 10,000 cells were injected into each recipient testis via the efferent duct, and each treatment was injected into the testes of 4 mice per replicate, with the contralateral testis receiving the alternate treatment. Recipient mice were culled at 2-month post-transplantation, and testes were collected and fixed. The number of LacZ expressing donor derived colonies of spermatogenesis was assessed using X-gal staining. 'SSC number' was reported as the number of colonies counter per 100,000 cells injected.

Assessment of epididymal sperm concentration, motility, and viability

To quantify sperm production and compare sperm quality (motility and viability) between untreated control and EPAS1-cKO mice, spermatozoa were collected from the caudal region of the epididymis using retrograde perfusion, as described previously.[47] Equal volumes of sperm

were collected from each mouse, then released into 1 mL of fixative and the number of sperm per mL calculated to produce a relative value that allowed for direct comparison between animals. For busulfan treated animals, retrograde perfusion was not possible due to the small size of the epididymides. For these experiments, the cauda epididymis was placed into 750 μL of modified Biggers Whitten, and Whittingham (BWW) media[48] containing 91.5 mM NaCl, 4.6 mM KCl, 1.7 mM $CaCl_2 2H_2O$, 1.2 mM KH_2PO_4, 1.2 mM $MgSO_4 7H_2O$, 25 mM $NaHCO_3$, 5.6 mM D-glucose, 0.27 mM sodium pyruvate, 44 mM sodium lactate, 5 U/mL penicillin, 5 μg/mL streptomycin, 20 mM HEPES buffer, and 3.0 mg/mL BSA) (pH 7.4; osmolarity 300 mOsm/kg). Three incisions were made, and sperm were allowed to 'swim out' for a 20 min period at 37°C, before collection, fixation, and quantification.

For the assessment of sperm parameters in untreated control and EPAS1-cKO mice, sperm were incubated in BWW for 20 min at 37°C, and total sperm motility, progressive motility, and viability were assessed. Total motility was assessed via microscope analysis, while progressive motility was assessed using Computer-Assisted Sperm Analysis (CASA), as previously described.[49] Total sperm viability was calculated via an eosin exclusion assay.

Daily sperm production assay

A daily sperm production (DSP) assay was conducted as described previously[30] to provide a quantitative measure of spermatogenesis to accompany epididymal sperm counts (described above). Briefly, snap-frozen mouse testes were solubilised using a detergent solution (0.9% sodium chloride, 0.01% azide, and 0.05% Triton X-100, all from Sigma Aldrich) and sonication, causing lysis to all cells except for the detergent-resistant elongated spermatids. Spermatid nuclei were then counted using a haemocytometer, and the number of sperm per gram of testis weight calculated. This value was then divided by 4.84 (the number of days that developing spermatids spend in the testis) to produce the DSP value.

Bulk RNA-seq

Undifferentiated spermatogonia from four independent cultures were treated with either vehicle (DMSO) or 250 μM Daprodustat, as described above (in 'primary cultures of undifferentiated spermatogonia'), before resuspension in Trizol reagent (ThermoFisher). Total RNA was extracted using a Direct-zol RNA Microprep kit (Zymo Research, CA, USA). Next, cDNA libraries were generated using Illumina poly(A) enrichment, and sequencing was performed using an Illumina NovaSeq 6000 at the Australian Genome Research Facility (AGRF, VIC, Australia). For each sample, 20–30 million reads of 150 base pairs in length were generated and aligned to the *Mus musculus* genome (mm39) using STAR aligner. Raw gene counts were calculated, and transcripts were assembled with the StringTie tool (v 2.1.4). EdgeR (v 3.38.4) was used to perform differential expression analysis. Gene expression is reported as average log count per million (logCPM) for the gene across all samples. Genes with a False Discovery Rate (FDR) value of <0.05 were considered to be significantly different between treatments. Gene Ontology analysis was performed on differentially expressed gene lists using DAVID Bioinformatics Resources (V6.8).[50,51]

Single cell RNA sequencing

To generate a scRNA-seq comparison of control and EPAS1-cKO spermatogonia in regenerative conditions, 2× control and 2× cKO male mice (6 weeks old) were pre-treated with low-dose busulfan (20 mg/kg). Testes were collected at 14 days post-busulfan treatment to capture undifferentiated spermatogonia within the window of time that they are known to be actively regenerating (Figure 4A).[19,31] A single cell suspension was created using Collagenase IA and 0.25% Trypsin-EDTA (as described above in 'flow cytometric analysis and cell sorting'). Enrichment of the undifferentiated spermatogonia population was then achieved via Magnetic Activated Cell Sorting (MACS) using a CD49f (α6-integrin) biotin-conjugated antibody (Miltenyi, North Rhine-Westphalia, Germany; #130-097-243, Table S2) paired with anti-biotin microbeads (Miltenyi, #130-090-485, Table S2). Immediately prior to the preparation of single-cell cDNA libraries, equal numbers of cells from each replicate were pooled to create a single control and a cKO population for analysis. Live cell populations were loaded into a Chromium Controller (10x Genomics Inc., CA, USA), and single-cell cDNA libraries were generated using v3 chemistry as per the manufacturer's instructions. Control and cKO libraries were then combined and sequenced in a single lane on an Illumina NovaSeq 6000 (Ramaciotti Center for Genomics, University of New South Wales, NSW, Australia). Raw base call files were demultiplexed using the RNA STARsolo pipeline and aligned to the mouse mm10 transcriptome.

Control and EPAS1-cKO transcriptomes were imported into Seurat and merged into a single object.[52] To ensure high quality data, cells with unique feature counts below 200 or above 8000 were excluded from further analysis. Testicular somatic cells that were carried over from the germ cell preparation were also excluded from further analyses, following their identification using well defined markers.[22] Merged germ cell datasets were then normalised and scaled using Seurat. The "FindVariableGenes" function was used to identify variable genes for principal component analysis. For clustering and UMAP graphing, 7 significant principal components were used (resolution set to 0.5). Gene Ontology was performed using the clusterProfiler package.[53,54]

Mining of previously published scRNA-seq datasets

To assess transcript levels of hypoxia-responsive transcription factors in spermatogonial sub-populations from the testis, analyses were conducted on a previously published scRNA-seq dataset containing spermatogonia from a PD6 mouse, which were isolated using a Rosa26-tdTomato^{flox_STOP_flox} transgene driven by *Blimp*-Cre expression (Law et al.,[21] GEO accession number GSE124904). The PD6 spermatogonia library was imported into Seurat, and the dataset was normalised and scaled, and the "FindVariableGenes" function was used to identify

variable genes for use in principal component analysis. For clustering and t-SNE graphing, 15 significant principal components were used (resolution set to 0.5).

QUANTIFICATION AND STATISTICAL ANALYSIS

Experiments were conducted a minimum of three times on biologically independent samples unless otherwise stated. Data are presented as Mean $\pm$ SEM. Statistical differences were established using the ANOVA or t-test function in GraphPad Prism 9 software. A value of $p < 0.05$ was considered to be statistically significant.